**Methane distribution and oxidation around the Lena Delta in summer 2013**

Ingeborg Bussmann, Steffen Hackbusch, Patrick Schaal, Antje Wichels

Alfred Wegener Institute for Polar and Marine Research, Marine Station Helgoland, Kupromenade 201, 27498 Helgoland, Germany

*Correspondence to*: Ingeborg Bussmann (Ingeborg.bussmann@awi.de)

**Abstract.** The Lena River is one of the biggest Russian rivers draining into the Laptev Sea. Due to predicted increasing temperatures, the permafrost areas surrounding the Lena Delta will melt at increasing rates. With this melting, high amounts of methane will reach the waters of the Lena and the adjacent Laptev Sea. Methane oxidation by methanotrophic bacteria is the only biological sink to reduce methane concentrations within the system. However, the polar estuary of the Lena River is a challenging environment for bacteria, with strong fluctuations in salinity and temperature. We determined the activity (tracer method) and the abundance (via qPCR-method) of aerobic methanotrophic bacteria. We described the methanotrophic population with MISA; as well as the methane distribution (via head-space method) and other abiotic parameters in the Lena Delta in September 2013.

In "riverine water" (S <5) we found a median methane concentration of 22 nmol $L^{-1}$, in "mixed water" (5 < S < 20) the median methane concentration was 19 nmol $L^{-1}$ and in "polar water" (S > 20) a median of 28 nmol $L^{-1}$ was observed. The Lena River was not the methane source for surface water, and bottom water methane concentrations were mainly influenced by the concentration in surface sediments. However, the methane oxidation rate in riverine and polar water was very similar (0.419 and 0.400 nmol $L^{-1}$ $d^{-1}$), but with a higher relative abundance of methanotrophs and a higher "estimated diversity" with respect to MISA OTUs in the "riverine water" as compared to "polar water". The turnover times of methane ranged from 167 d in "mixed water", 91 d in "riverine water" to only 36 d in "polar water". Also the environmental parameters influencing the methane oxidation rate and the methanotrophic population differed between the water masses. Thus we postulate a riverine methanotrophic population limited by sub-optimal temperatures and substrate concentrations and a polar methanotrophic population being well adapted to the cold and methane poor environment, but limited by the nitrogen content. The diffusive methane flux into the atmosphere ranged from 4 - 163 $\mu$mol $m^2$ $d^{-1}$ (median 24). For the total methane inventory of the investigated area, the diffusive methane flux was responsible for 8% loss, compared to only 1% of the methane consumed by the methanotrophic bacteria within the system. Our results underscore the importance of measuring the methane oxidation activities in polar estuaries and indicate a population-level adaptation of the water column methanotrophs to riverine versus polar conditions.

## 1    Introduction

Methane is an important greenhouse gas and strong efforts are ongoing to assess its different sinks and sources. Methane sources and sinks vary with latitude (Saunois et al., 2016). Overall, about two-thirds of the emissions are caused by human activities; the remaining third is from natural sources (Kirschke et al., 2013). At polar latitudes, methane sources include wetlands, natural gas wells and pipelines, thawing permafrost, and methane hydrate associated with decaying offshore permafrost (Nisbet et al., 2014). To resolve the divergence between

top-down and bottom up estimates of methane sources more data are needed, but the measurement network for methane concentration and isotopes is very thin (Nisbet et al., 2014). Spatially and temporally, better measurements are essential to identify and quantify methane sources.

The Arctic Ocean is an intercontinental sea surrounded by the landmasses of Alaska/U.S.A., Canada, Greenland,
45 Norway, Iceland, and Siberia/Russia. It represents about 1% of the global ocean volume but receives about 10% of global runoff (Lammers et al., 2001). It has a central deep basin and is characterized by extensive shallow shelf areas including the Barents Sea, Kara Sea, Laptev Sea, East Siberian Sea, Chukchi Sea, and Beaufort Sea. The sources of methane in the arctic may be from thawing methane hydrates off Svalbard (Westbrook et al., 2009), and ebullition of methane from diverse geologic sources (Mau et al., 2017; Shakhova et al., 2014). In
50 addition, extensive shallow-water areas of the Arctic continental shelf are underlain by permafrost, which was formed under terrestrial conditions and was subsequently submerged by post-glacial rise in sea level. Methane can be trapped within this permafrost, as well as below its base (Rachold et al., 2007).

The further fate of methane depends on several factors. When methane leaves the sediment (either by diffusion or by ebullition) at depths > 200 m, most of it will be dissolved into the water below the thermocline and will not
55 reach surface waters or the atmosphere (Gentz et al., 2013; Myhre et al., 2016). However, ebullition at shallow water depths represents a short cut as it will not dissolve into the water, and most of this methane will reach the atmosphere. For lakes, it has been estimated that ebullition contributed to 18-22% of the total emission (Del Sontro et al. 2016). Only methane dissolved in the water can be oxidized by certain methane oxidizing bacteria (MOB). They convert methane to $CO_2$ and water, and thus can reduce its greenhouse effect considerably
60 (Murrell and Jetten, 2009). Water column methane oxidation (MOX) is consequently the final sink for methane before its release to the atmosphere. The amount of methane consumed by this microbial filter depends on their abundance and the water current pattern (Steinle et al., 2015). But mostly methane concentrations and temperature determine their efficiency (Lofton et al., 2014). However, not much is known about the abundance and population structure of marine, polar MOBs.
65 Especially the area of the Laptev and East Siberian Sea has been in the scientific focus. In certain studies the partial thawing of permafrost on the shallow East Siberian Arctic Shelf is considered to be responsible for very high dissolved methane concentrations in the water column (> 500 nmol L$^{-1}$) and elevated methane concentrations in the atmosphere (Shakhova et al., 2014). Other authors have shown that, in the Laptev Sea, methane released from thawing permafrost is efficiently oxidised by microorganisms in the overlying unfrozen
70 sediments, such that methane concentrations in the water column were close to normal background levels (Overduin et al., 2015). High-resolution simultaneous measurements of methane in the atmosphere and above surface waters of the Laptev and East Siberian Seas revealed that the sea-air methane flux is dominated by diffusive fluxes, not bubble fluxes (Thornton et al., 2016).

The aim of this study was to get an overview of the methane distribution in the near shore parts of the Laptev
75 Sea and to gain insight into the role of methane oxidizing bacteria in the methane cycle in this area. Furthermore, we tried to assess which environmental factors determine the methane distribution and its oxidation.

## 2    Material and Methods

### 2.1    Study site

80 The Lena Expedition was conducted in late summer, 1–7 September 2013 on board the Russian R/V "Dalnie Zelentsy" of the Murmansk Marine Biological Institute, in the surrounding areas of the Lena River Delta region,

Laptev Sea, Siberia. Four transects around the Lena Delta were investigated (Figure 1). Transect 1 started near the peninsular Bykovski and headed towards the northeast. This transect was the same as in 2010 (Bussmann, 2013a). Transect 4 was located near the mouth of the Trofimovskaya Channel and Transect 6 located at the

85      northern point of the Delta. Hydrography (temperature, salinity, currents) and water chemistry (DOC, pH, oxygen, TDN) were determined as described in (Gonçalves-Araujo et al., 2015; Dubinenkov et al., 2015). Water samples were taken using Niskin bottles at surface and discrete depths chosen based on CTD profiles. Samples for methane analyses were taken from surface and bottom waters, and at deeper stations also at the pycnoclines. Sediment surface was sampled with a grab sampler.

90      We classified the water masses as follows „riverine water" with a salinity < 5, "mixed water" with 5 < S < 20 and „polar water" with a salinity > 20, modified from (Caspers, 1959).

## 2.2     Water sampling and gas analysis

Duplicate serum bottles (120 ml) were filled with thin silicon tubing from the water sampler. The bottles were

95      flushed extensively with sample water (to ensure no contact with the atmosphere) and finally closed with butyl rubber stoppers; excess water could escape via a needle in the stopper. Samples were poisoned with 0.3 ml of 25% $H_2SO_4$. In the home laboratory, 20 ml of nitrogen were added to extract methane from the water phase, and excess water could escape via a needle. The samples were vigorously shaken and equilibrated for at least two hours. The volumes of the water and gas phases were calculated by differential weighing.

100     For sediment samples, 3 ml of surface sediment was filled with cut off syringes into 12 ml glass ampoules. The samples were poisoned with 2 ml NaOH and sealed with butyl rubber stoppers.

Headspace methane concentrations were analysed in the home laboratory with a gas chromatograph (GC 2014, Shimadzu) equipped with a flame ionisation detector and a molecular sieve column (Hay Sep N, 80/100, Alltech). The temperatures of the oven, the injector and detector were 40°C, 120°C and 160°C, respectively. The

105     carrier gas ($N_2$) flow was 20 ml min$^{-1}$, with 40 ml min$^{-1}$ $H_2$ and 400 ml min$^{-1}$ synthetic air. Gas standards (Air Liquide) with methane concentrations of 10 and 100 ppm were used for calibration. The calculation of the methane concentration was performed according to Magen et al., (2014), taking into account the different methane solubilities at the wide range of salinities (1 – 33). The precision of the calibration line was $r^2 = 0,99$, the reproducibility of the samples 7%. The methane related data set is available at www.pangaea.de,

110     doi:10.1594/PANGAEA.868494, 2016.

## 2.3     Determination of the methane oxidation rate (MOX)

The MOX rate was determined as described in Bussmann et al., (2015). After filling triplicate sample bottles and one control bottle, a diluted tracer (0.1 ml of $^3$H-CH$_4$, American Radiolabeled Chemicals) was added to the

115     samples (2 kBq ml$^{-1}$). Samples were shaken vigorously and incubated for 24 hours in the dark at near in situ temperatures (approximately 4 - 10°C). After incubation, methane oxidation was stopped by adding 0.3 ml of 25%$H_2SO_4$. Controls were stopped before the addition of the tracer. The principle of the MOX rate estimation is the comparison between the total amount of radioactivity added to the water sample and the radioactive water that was produced due to oxidation of the tritiated methane. The ratio between these values corrected for the

120     incubation time is the fractional turnover rate (k'; d$^{-1}$). The in situ MOX rate (nmol L$^{-1}$ d$^{-1}$) is then obtained by multiplying k' with the in situ methane concentration. Additionally, we calculated the turnover time (1 /k'), i.e. the time it would take to oxidize all the methane at a given MOX rate, assuming that methane oxidation is a first-

order reaction. To determine the total radioactivity of the sample and the radioactivity of the tritiated water, 4-ml aliquots of water were mixed with 10 ml of the scintillation cocktail (Ultima Gold LLT, Perkin Elmer) and analysed with a liquid scintillation counter (Beckman LS 6500). The limit of detection was calculated as described in Bussmann et al., (2015) and was determined to be 0.028 nmol L$^{-1}$ d$^{-1}$ for this data set.

### 2.4 PCR amplification of methane monooxygenase genes

Samples (250 ml) from surface and bottom water were filtered through 0.2 $\mu$m cellulose acetate filters (Sartorius) and stored frozen until further processing. High molecular weight DNA was extracted following the protocol of PowerWater® DNA Isolation Kit (MoBio). DNA concentrations were determined photometrical (TECAN infinite200). Each sample DNA was checked for the presence of methanotrophic DNA with the primers wcpmoA189f / wcpmoA661r, as water column-specific primers (Tavormina et al., 2008). Each PCR reaction (30 $\mu$l) contained 2 U of Taq Polymerase (5 Prime), 3 $\mu$l PCR Buffer (10x), 6 $\mu$l PCR Master Enhancer (5 ×), 200 $\mu$M dNTP Mix (10 mM Promega), 0.6 $\mu$M of each primer, and 10 ng of DNA template. Initial denaturation at 92°C for 180 s was followed by 30 cycles of denaturation at 92°C for 30 s, annealing at 59°C for 60 s and elongation at 72°C for 30 s. The final elongation step was at 68°C for 300 s. Successful amplification was confirmed by gel electrophoresis on a 1.5% (w/v) agarose gel.

### 2.5 Quantitative PCR (qPCR) of methane monooxygenase genes

Extracted DNA from each sample was amplified by qPCR using a LigthCycler R 480 (Roche, Germany) and master mixes from the company (Roche, Germany). Each sample was measured in triplicate.

A pure culture of *Methylobacter luteus* (NCIMB 11914) was used to construct standard curves for total *pmoA* gene. Cell numbers of the *M. luteus* cultures were determined microscopically (DAPI) and after extraction DNA was quantified using a TECAN infinite M200 spectrophotometer (TECAN, Switzerland). A serial dilution of DNA (equivalent to $10 - 10^6$ cells ml$^{-1}$) was used to construct standard curves. Correlation coefficients of standard curves were > 0.98.

The qPCR reaction mix (20 $\mu$l) contained 10 $\mu$l Master Mix (2 x LightCycler® 480 kit hot-start SYBR Green I Master, Roche, Germany), 10 mM of each PCR-primer (as described above) and 5 $\mu$l template DNA. The amplification was performed with an initial denaturation step at 95 °C for 5 min, followed by 45 cycles of denaturation at 95 °C for 10 s, annealing at 59 °C for 60 s and extension at 72 °C for 30 s. Fluorescence data were acquired during an additional temperature step (60 s at 65 °C).

### 2.6 Methane monooxygenase intergenic spacer analysis (MISA)

All samples showing *pmoA* genes were analysed with MISA to differentiate the methanotrophic populations and describe their "estimated diversity" by analysing the differences in the composition of methane monooxygenase genes with regard to their geographical distribution (Tavormina et al., 2010).

The PCR master mix (20 µl) contained 200 $\mu$M dNTPs, (Promega), 2 U Taq DNA polymerase (5 Prime), 2 $\mu$l PCR Buffer (10x), 4 $\mu$l PCR Master Enhancer (5 ×), and 15 ng target DNA. Two PCR runs were carried out with a MasterCycler gradient (Eppendorf, Germany) modified after Tavormina et al., (2010) using two sets of primers (Thermo Fisher Scientific GmbH, Germany): To enrich *pmoA* sequences from bulk environmental DNA primers spacer_pmoC599f (5'-AAYGARTGGGGHCAYRCBTTC), spacer_pmoA192r (5'-TCDGMCCARAARTCCCARTC) were used. In a second round of semi-nested amplification the primers

spacer_pmoC626_IRD (5'-RCBTTCTGGHTBATGGAAGA), and spacer_pmoA189r (5'-CCARAARTCCCARTCNCC) were used with purified PCR product from the first PCR as template. Primer spacer_pmoC626_IRD is labelled with an infrared Dye (Dy 682 nm) for the detection of amplified products using a Licor DNA Analyzer 4300 system (Licor, Germany). Primers are modified versions of MISA primers as reported in Tavormina et al., (2010). Modifications used in the current work increased amplicon strength and recovery of diverged lineages (Tavormina, pers comm). In detail, after an initial denaturation at 94°C for 180 s, 30 cycles of denaturation at 94°C for 30 s, annealing at 52°C for 60 s and elongation at 72°C for 30 s followed in the first PCR. The final elongation step was at 72°C for 300 s. In the second PCR 2 $\mu$l of purified PCR product of the first PCR was used for amplification with modified and labelled primers (see above). The PCR program was modified as follows: after initial denaturation at 94°C for 180 s, 5 cycles of denaturation at 94°C for 30 s, annealing at 52°C for 60 s and elongation at 72°C for 30 s and 25 cycles with an annealing temperature of 48°C. Amplified samples were separated on polyacrylamid gels using a DNA Analyzer 4300 (Licor, Germany). Running conditions on a 6.5% polyacrylamid gel (Lonza, Switzerland, 25 cm length, 0.25 mm thickness) were 1500 Volt, 40 mA, 40 W for 3.30 h at 45 °C. A 50-700 bp sizing standard (IRDye 700, Licor, Germany) was applied on the gel. For the analysis of the MISA fingerprints (Bionumerics 7.0, Applied Maths, Belgium) size fragments of 350 to 700 bp were included (Schaal, 2016). Binning to band classes was performed with a position tolerance setting of 1.88%. Each band class is referred to as a MISA operational taxonomic unit (MISA-OTU). Band patterns of MISA-OTUs were translated to binary data reflecting the presence or absence of the respective OTU.

### 2.7    Calculation of the diffusive methane flux

The gas exchange across an air–water interface can be described in general by the following function (Lisa and Slater, 1974; Wanninkhof et al., 2009):

$$F = k_{CH4} * (c_m - c_{equ})$$

where F is the rate of gas flux per unit area (mol m$^{-2}$ d$^{-1}$), $c_m$ is the methane concentration measured in surface water and $c_{equ}$ is the atmospheric gas equilibrium concentration based on Wiesenburg and Guinasso (1979). Data on the atmospheric methane concentration were obtained from the meteorological station in Tiksi via NOAA, Earth System Research Laboratory, Global Monitoring Division (http://www.esrl.noaa.gov/gmd/dv/iadv/). The gas exchange coefficient (k) is a function of water surface agitation. The k value in oceans and estuaries is more determined by wind speed, while in rivers water velocity dominates (Alin et al., 2011). The determination of k is very important for the calculation of the sea-air flux. We decided to calculate $k_{600}$ in the in the Laptev Sea according to the following equation, developed for coastal seas by Nightingale et al. (2000).

$$k_{600} = 0.333 \, U_{10} + 0.222 \, U_{10}^2$$

Wind data ($U_{10}$) were obtained for Tiksi from the „Archive of Tiksi for Standard Meteorological Observations" Institute (2016) For the flux calculation the median wind speed of each day was used. The calculated $k_{600}$ (value for $CO_2$ at 20°C) was converted to $k_{CH4}$ according to Striegl et al., (2012), where Schmidt numbers (Sc) are determined by water temperature and salinity (Wanninkhof, 2014).

$$k_{CH4} / k_{600} = (Sc_{CH4} / Sc_{CO2})^{0.5}$$

To estimate the role of methane oxidation and diffusive methane flux for the methane inventory in the Lena Delta we made the following calculations. The area was divided into two squares, which surrounded our station grid (Appendix Figure A1). The median depth from the stations within each of these squares was 13 m. Based on the longitude / latitude of the squares we calculated the area and then the volume of each square ($1.3 \times 10^{11}\,m^3$ and $2.5 \times 10^{11}\,m^3$). With the median methane concentration and median MOX of all stations within each square, we calculated the total methane inventory of the investigated areas (in mol, sum of both squares), as well as the total methane oxidation rate (mol / d). The total diffusive flux (in mol / d) of the region was obtained by multiplying the median diffusive flux of all stations with the total area.

### 2.8 Statistical analysis

To test for differences between the different water masses we applied a one-way ANOVA with log transformed data (Kaleidagraph (4.3). To test for differences between different groups we used the non-parametric Wilcoxon or Kruskal Wallis test (Kaleidagraph (4.3). The linear correlation analyses were performed with StatPlus, AnalystSoft Inc. Version v6.

## 3 Results

### 3.1 Hydrography

We grouped our sampling stations into "riverine water" with a salinity < 5. In this water mass the median salinity was 2.45, ranging from 0.8 – 4.8. Median temperature was 9.8°C, ranging from 7.3 – 11.4°C. In the "mixed water" the median salinity was 11.4, ranging from 5 – 19.7. Median temperature was 6.4°C, ranging from 2.5 – 8.8°C. In the "polar water" the median salinity was 27.2, ranging from 21.5 – 33.2. Median temperature was 3.0°C, ranging from 1.8 – 6.2°C. In September 2013 we observed a sharp stratification with warm freshwater at the surface (0 – 5 m), followed by a mixed water body. Below approx.10 m water depth, we found cold and saline water (= polar water). As example of this sharp stratification, the salinity distribution of Transect 1 is shown in Figure 2a. The freshwater plume was most pronounced in Transect 4 and 5 and extended far to the north (Appendix Figure A2). In Transect 6 only the first near-shore station had riverine water, the following stations were already characterized by polar waters.

### 3.2 Methane concentrations

Methane concentrations around the Lena Delta showed elevated concentrations near shore and decreased with distance from the shore (Figure 3). This decrease off the coast was most distinct for the Transect 1 and 4, where also the maximal concentrations (218 nmol $L^{-1}$) were observed. In contrast, methane concentrations were distributed rather uniform in the northern Transect 6. At station TIII-1304 (pale orange in Figure 3) we observed very high methane concentrations in surface and bottom water. No clear pattern in the depth distribution of methane was observed (Figure 2b). Methane concentrations of the sediment surface ranged from 0.4 $\mu$M at the eastern station of Transect 4 and 5.4 $\mu$M at the beginning of Transect 1 (median of 2.07 $\mu$M).

When applying our water masses (riverine, mixed and polar), we observed significantly different methane concentrations in these water masses, with medians of 22, 19 and 26 (p = 0.03) respectively (Table).

In „riverine water", methane concentration was significantly correlated with temperature ($r^2 = 0.38$, Appendix Table A1) and negatively correlated with the oxygen concentration ($r^2 = 0.73$). In „mixed water", we found a

weak but significant correlation between methane and TDN ($r^2 = 0.27$, Appendix Table A1). In „polar water" the methane concentration of the water column was significantly correlated with the methane concentration in the surface sediment ($r^2 = 0.33$). The influence of the sediment methane concentration on the water column

245     concentration was even more pronounced when taking all bottom water samples (=„polar water" + one "mixed water" + one "riverine"sample) and excluding the very high water values of station TIII-1304; hereby the correlation was much stronger ($r^2 = 0.62$, n= 33, Figure 4).

### 3.3     Methane oxidation rate (MOX) and fractional turnover (k')

250     Methane oxidation rates ranged from below the detection limit (< 0.028 nmol $L^{-1}d^{-1}$, with 8.7% of the data) up to 5.7 nmol $L^{-1} d^{-1}$. In „riverine" and „polar water" methane oxidation was rather high (median of 0.419 and 0.400 nmol $L^{-1}$ $d^{-1}$) versus low rates in „mixed water" (median of 0.089 nmol $L^{-1}d^{-1}$, Table). On a spatial range, we observed slightly elevated rates near the coast, at the beginning of the Transects 1 and 4 (Figure 5a). In the bottom waters elevated values were observed near the coast, at the beginning of Transects 4 and 5.

255     In the „riverine water" MOX was significantly correlated with temperature ($r^2 = 0.77$, Appendix Table A2). In „mixed water" none of the measured parameters was of any significance. In „polar water", TDN explained 31% of the observed MOX variability. In all water masses, MOX was influenced by the methane concentration, but the influence was strongest in „riverine water" ($r^2 = 0.98$) and decreased towards mixed and polar water ($r^2 = 0.80$ and 0.56 respectively, Appendix Table A2). However, as MOX is calculated with the methane

260     concentration, this correlation has to be regarded with caution.

The fractional turnover (k') is a measure for the relative activity of the MOBs and it is independent of the methane concentration. We observed significantly different k' in riverine, mixed and polar water with highest k' in "polar water" (median of 0.011, 0.006 and 0.028 $d^{-1}$ respectively, Table). Temperature was most important for the k' in riverine water ($r^2 = 0.84$, Appendix Table A2). In "mixed water", salinity and TDN correlated with k'

265     ($r^2 = 0.46$ and 0.37 respectively). In "polar water", none of our parameters was of any importance.

### 3.4     Relative abundance of methane oxidizing bacteria

The abundance of MOB can either be given in cell numbers or as relative abundance. Cell numbers ranged from 4.0 x $10^4$ – 4.6 x $10^5$ cells per L, except station T1-1302 with very high numbers of 2 and 3 x $10^6$ cells per L. The

270     relative abundance (relating the MOB-DNA to the total extracted DNA) ranged from 0.05 – 0.47%, except the high values from station T1-1302 with 1.69 and 2.63% (surface and bottom respectively, Figure 6). The detection limit was 3.2 x $10^4$ cells / L, and about ¼ of the samples was below this limit.

The relative abundance of MOB was significantly different between riverine, mixed and polar water (Table). In "riverine" water the highest relative abundance was observed, decreasing towards the "polar water" (median

275     values of 0.81%, 0.19% and 0.03% respectively).

For further analysis, we excluded the outliers with their very high values and as the total number of data was small (n = 18) we performed a linear regression analysis with all values (no separation of the different water masses). None of the methane related parameters (methane concentration, MOX and k') could explain the observed relative abundance of MOBs. However, the relative abundance of MOBs was significantly and

280     positively correlated with DOC and temperature ($r^2 = 0.52$; p = 0.0002 and $r^2 = 0.41$; p = 0.0002), as well as negatively correlated with salinity ($r^2 = 0.47$; p <0.0001). Additionally, "estimated diversity" as OTUs per

station showed a weak but significant correlation with relative abundance ($r^2 = 0.20$; $p = 0.04$). Similar results were obtained with the cell numbers as dependant parameter.

### 3.5 Methanotrophic population

With the MISA fingerprinting method, we could detect 9 different OTUs. These OTUs were named according to their PCR fragment length (size in bp). However, two OTUs (420 and 506) were observed at all stations and all depths. Thus their occurrence pattern could not give any ecological information and they were excluded from further analysis.

The "estimated diversity" of MOBs, as number of OTUs per station was significantly different between riverine, mixed and polar waters, with 4, 3 and 2 OTUs per station respectively (Kruskal Wallis test, $p = 0.02$, Table 2). The Kruskal-Wallis test was applied for each OTU (presence / absence data) to analyse the association with the three water masses. OTU-557 showed a clear association with polar water ($p = 0.06$), while OTU-460 and OTU-398 were not found in polar water. OTU-535 showed a significant association with river and mixed water ($p=0.02$), as well as OTU-362 (even though not significant). OTU-485 and OTU-445 showed no clear association. With respect to the PCR fragment size, some of the OTUs have been described before (Tavormina et al., 2010), thus OTU-535 could be assigned to Group Z, OTU-485 to *Methylococcus capsulatus, Methylohalobius crimeensis* and OTU-445 to OPU-1 (Table 2).

### 3.6 Diffusive methane flux

To calculate the diffusive flux of methane we need information on the atmospheric methane concentration as well as the wind speed for the respective dates, as outlined in the Material & Method section. The atmospheric methane concentration ranged from 1.896 – 1.911 ppm $CH_4$. The wind in September 2013 was rather low with 4.2 ± 2.2 m/s. The calculated values for $k_{600}$ ranged from 0.37 to 3.17 m d$^{-1}$ with a median of 1.05 m d$^{-1}$, while $k_{CH4}$ ranged from 0.52 to 4.51 m d$^{-1}$ with a median of 1.43 m d$^{-1}$.

The diffusive flux of methane into the atmosphere was rather low for the Transects 1, 5 and 6 with median values of 31, 8 and 13 $\mu$mol m$^{-2}$ d$^{-1}$, compared to a median flux of 163 $\mu$mol m$^{-2}$ d$^{-1}$ for Transect 4. The highest flux was observed at the near shore stations of Transect 4 with 478 and 593 $\mu$mol m$^{-2}$ d$^{-1}$; this was mainly due to higher methane concentrations (118 and 151 $\mu$M) and higher wind speed at the sampling day.

Our cruise covered a total area of 3051 km$^2$ (Appendix Figure A1), with an inventory of 10161 kmol methane. Based on our estimations about 822 kmol per day (median valued of all stations) diffused into the atmosphere, while 118 kmol per day (median valued of all stations) were oxidized. Thus about 8% of the total methane inventory leaves the aquatic system via diffusion, while only 1% could be oxidized each day.

## 4 Discussion

### 4.1 Methane concentrations

In the coastal area of the Laptev Sea we observed rather low methane concentrations (overall median 25 nmol L$^{-1}$, ranging from 10 – 218 nmol L$^{-1}$). Transect 1 was located at the same positions as in our expedition in 2010 (Bussmann, 2013b). Near shore, methane concentrations were slightly higher in 2013, but overall, there was no significant difference (Wilcoxon Rank Sign Test for paired data, $n = 18$, $p = 0.84$). In the same study area and in summer 2014, other authors reports a range of 10 – 100 nmol L$^{-1}$ (estimated from Figure 2 in Sapart et al., 2017). At station TIII-1304 rather high methane concentrations were observed. We attribute this to the fact that at the

sampling time the wind had strongly increased. (Afterwards sampling had to be stopped). Thus sediment resuspension in this shallow water and methane release from the sediment might be the reason for these high methane concentrations (Bussmann, 2005). On the other hand, for this region highly active methane seeps are also reported (Shakhova et al., 2014) and methane ebullition could also be a reason for the high methane concentrations. Unfortunately for our cruise no sonar data were available, thus we do not have any information on seep activity.

The water masses we had classified were separated by a strong pycnocline. Thus also different parameters influenced the corresponding methane distribution. In riverine water methane concentrations were correlated positively to temperature and negatively to oxygen concentration. This correlation can be related to degradation processes finally leading to methanogenesis, which are enhanced by temperature and are consuming oxygen. The removal of DOM occurs primarily at the surface layer, which is likely driven by photodegradation and flocculation (Gonçalves-Araujo et al., 2015). Beside the degradation of DOM, dimethylsulfoniopropionate (DMSP) as osmoprotectant and antioxidant of microalgae could also lead to in situ methane production (Florez-Leiva et al., 2013).

Another source of methane might be the water of the Lena River. Methane concentrations in the Bykowski Channel of the Lena River are on average $58 \pm 19$ nmol $L^{-1}$ (Bussmann 2013 and unpublished data from 2012 and 2016). This is much lower than the average global riverine methane concentration of $1350 \pm 5160$ nmol $L^{-1}$ (Stanley et al., 2016). However, for the estuaries of other arctic estuaries - Ob and Yenisei - similar low concentrations are reported; $18 \pm 16$ nmol $L^{-1}$ from Savvichev et al. (2010) and approx. 30 nmol $L^{-1}$ from Kodina et al. (2008). We did find elevated methane concentrations near the coast. However, no correlation between salinity and methane concentration i.e. a dilution of methane-rich river water with methane-poor marine water was observed (neither for the separate water masses nor for the whole data set). This is also confirmed by our previous study (Bussmann, 2013b) and we thus exclude the Lena River as methane source.

One reason for this missing correlation, could be another source of freshwater, but with low methane concentrations. In contrast to other estuaries, arctic estuaries are ice covered about 2/3 of the year and the seasonal freezing and melting of ice has a strong impact on the water budget. The freezing of sea water results in brine formation with strongly increased salinity, while its melting results in a freshwater input (Eicken et al., 2005). To a lesser extent this holds also true for freshwater ice. In 1999, the river water fraction in ice-cores near our study area ranged from 57% - 88% (Eicken et al., 2005), thus we expect additional non-river-freshwater input. Even though not much is known about methane concentrations in ice, based on a recent study on sea-ice in the East Siberian Sea (Damm et al., 2015), we assume that this melt water probably has lower methane concentrations than the river-freshwater. This additional aspect of the water budget in ice covered estuaries might explain the missing relation between salinity and methane concentration.

In bottom water, methane concentrations were only influenced by the methane concentration in the sediment below. Thus we assume that this methane mostly originates from a (diffusive) methane flux out of the sediment. In the shallow Chucki Sea methane the most likely methane source was also seafloor methanogenesis resulting from the decomposition of organic carbon (Fenwick et al.; 2017). Another source of methane to bottom waters is submarine groundwater discharge, as has been shown for two Alaskan sites (Lecher et al., 2019). However, low tides, low topographic relief, and low precipitation in the study area are not favourable for a high ground water

input in the Lena Delta. Unfortunately, no isotope analysis to validate the origin of the bottom water methane was possible.

### 4.2 Methanotrophic activity and the methanotrophic population

We measured an overall median methane oxidation rate of 0.32 nmol $L^{-1}$ $d^{-1}$, ranging from 0.028 – 5.7. In other coastal seas comparable values were observed with a median of 0.82 and 0.16 nmol $L^{-1}$ $d^{-1}$ for the coastal and marine part of the North Sea respectively (Osudar et al., 2015), and 0.1 nmol $L^{-1}$ $d^{-1}$ at the surface of the central North Sea (Mau et al., 2015) and 1 -11 nmol $L^{-1}$ $d^{-1}$ for Eckernförde Bay in the Baltic Sea (Steinle et al., 2017). In polar waters, off Svalbard and unaffected from ebullition sites, values of 0.26 -0.68 nmol $L^{-1}$ $d^{-1}$ (Mau et al., 2017) and 0.5 ± 1 nmol $L^{-1}$ $d^{-1}$ (Steinle et al., 2015) are reported. Thus our values are well within the reported range of polar and marine MOX. However, at the source of the „riverine water" i.e. the Lena River itself, much higher MOX (median = 24 nmol $L^{-1}$ $d^{-1}$) have been observed (Osudar et al., 2016). The first order rate constant used for modelling the methane flux in the Laptev Sea are estimated to range from 18116 $d^{-1}$ to 11 $d^{-1}$ (= 2.3 x $10^{-6}$ - 3.8 x $10^{-3}$ $h^{-1}$) (Wahlström and Meier, 2014). From our data we suggest more realistic turnover times ranging from 91 $d^{-1}$ in riverine water, 167 $d^{-1}$ in the mixed water and 36 $d^{-1}$ in polar water.

In the „riverine water", MOX and fractional turnover rates were correlated with temperature (ranging from 7 – 11°C), while in the other water masses no such correlation was found. Also, the influence of the methane concentration on the MOX was most pronounced in "riverine water" ($r^2$ = 0.98). In polar water, MOX was influenced the by TDN, but compared with riverine water, methane concentration had a much lower influence ($r^2$ = 0.56).

With the described method of qPCR and the water column specific primers from Tavormina et al., (2008), the relative abundance of MOB in our study ranged from 0.05 – 0.47% (median 0.16%) which is equivalent to 4 x $10^4$ – 3 x $10^6$ cells per L (median of 6.3 x $10^4$), except the high values from station T1-1302. These high values could not be explained by any environmental or methane-related parameters; thus they are regarded as methodological outliers. In a marine non-methane-seep area 2 – 90 copies of MOB-DNA per ml, equivalent to 1-45 x $10^3$ cells / L are reported (Tavormina et al., 2010) (assuming two copies of the pmoA gene per cell (Kolb et al., 2003)). In the Lena River the number of MOBs ranges 1 - 8 x $10^3$ cells / L (Osudar et al., 2016). In the boreal North Sea a broad range of 0.2 x $10^3$ – 8 x $10^8$ cells / L were found (Hackbusch, 2014). All of these studies had used qPCR with the same primes as we did. Thus our numbers are within the upper range of the reported values. When using CARD-FISH, the number of MOBs seem to be higher, with 3 – 30 x $10^6$ MOB cells /L in polar waters off Svalbard (Steinle et al., 2015) and 1 x $10^6$ cell / L at surface waters at the Coal Oil Point seep field in California (Schmale et al., 2015).

We found no correlation of cell numbers or relative abundance of MOB to methane related parameters (methane concentration, MOX and k'), but correlations to parameters important to heterotrophic bacteria, as amount of organic carbon, temperature and salinity (Lucas et al., 2016). Thus we have to assume, that with our qPCR we detected also cells, which were not active. This is supported by the finding that when MOX was not detectable, we still detected MOB-DNA in our samples. And vice versa, when MOB-DNA was not detectable we still could measure their activity (MOX). This could be due to the fact that there are MOB which were probably not amplified. The primer set used in this study is the most frequently used, however a couple of different primer sets are available for amplification of specific monooxygenase genes in several subgroups, which are not targeted using this primer set (Knief, 2015). Thus, these subgroups e.g. *Verrucomicrobia* or the anaerobic

methanotrophic bacteria of the NC10 phylum and others (Knief, 2015) were not quantified in our study.

405 Additionally, there might be dormant MOB present, whose DNA we detected, even though the cells were not active (Krause et al., 2012). Thus we can state, that the different water masses had significantly different abundances of MOB, with the highest in "riverine water" and the lowest abundance in "polar water".

With the method of MISA, we successfully applied for the first time a fingerprinting method to the

410 methanotrophic population in a polar estuary. However, there is actually only one study applying MISA to environmental samples. Two OTUs have been described in a marine study (Tavormina et al., 2010). The first group, OTU-1 has a broad distribution and belongs to the known group of gammaproteobacteria and also OTU-445, assigned to group OTU-1 was distributed equally in all different water masses we analysed. Group-Z is described as being not so abundant and belongs to a group of MOB of unknown lineage and function

415 (Tavormina et al., 2010). In this study, OTU-535 which was assigned to the Group-Z preferred the non-polar environment. OTU-485, which is assigned to the group of *Methylococcu*s, showed no specific association. Thus we conclude, that the methanotrophic populations in polar versus river/mixed water are different, with some OTUs not occurring in polar water and one OTU with a clear association with polar water. The populations in riverine and mixed water were very similar. Since a subset of OTUs identified in this study cannot be linked to

420 known MOBs, further attempts to isolate and describe new unknown polar MOB would be helpful to learn more about the diversity and the potential of these MOBs, but this is a challenging task. Further insight could also be obtained by next generation sequencing which gives an in deep view into population structure. Meta-genome and meta-transcriptome analyses could help to identify functional genes and reveal which types are really active and which are dormant.

425

Thus the ecological traits can be described as follows: we observed two distinct methanotrophic populations with different characteristic in the riverine versus polar water mass. In polar water, the methanotrophic activity was limited (influenced) by the nitrogen content and hardly by methane concentration. The relative abundance and "estimated diversity" (OTU/sample) of MOB was lower than in riverine water. Thus this polar population was

430 well adapted to the cold and methane poor environment, but limited by the nitrogen content. With their lower relative abundance and lower "estimated diversity", they were quite efficient in reaching a MOX comparable to riverine water. In the riverine water, the methanotrophic activity was limited by temperature and methane concentrations. The relative abundance and "estimated diversity" (OTU/sample) of MOB was higher than in polar water, even though the same MOX was measured. Thus this riverine population was not very efficient at

435 sub-optimal temperatures and substrate concentrations.

Methane concentration and nitrogen availability are strong driving forces shaping MOB community composition and activity (Ho et al., 2013). Furthermore the interactions with other heterotrophic bacteria influence the methanotrophic community (Ho et al., 2014). As DOM removal and degradation occurs mainly at the surface / riverine water (Gonçalves-Araujo et al., 2015); this may also lead to an enriched methanotrophic population in

440 the riverine water. We also assume that the riverine environment is exposed to more environmental changes (salinity, light, temperature) than the polar one. Changes in salinity have different impact on sensitive and non-sensitive MOBs, thus also shaping the methanotrophic community (Osudar et al., in revision). In contrast to our more divers riverine population, the methanotrophic population in the proper Lena river was characterized by a rather homogenous community (Osudar et al., 2016). However, the classical concept of r- and k-strategist

445    nowadays has been replaced by the C-S-R functional classification framework and type Ia MOB, responding rapidly to substrate availability and being the predominantly active community in many environments can thus be classified as competitors (C) and competitors-ruderals (C-R) (Ho et al., 2013).

### 4.3    Diffusive methane flux

450    For the calculation of the diffusive methane flux several parameters are necessary. The atmospheric methane concentrations as obtained from the database ranged from 1.896 to 1.911 ppm. This is a bit lower than 1.879 for the outer ice free Laptev Sea in summer 2014 as reported from Thornton et al., (2016). In contrast, our wind speed was a bit higher (4.2 ± 2.2 m/s) than 2.9 ± 1.9 m/s as reported from Thornton et al., (2016). This would result in slightly higher equilibrium concentrations and higher gas exchange coefficient in our study.

455    More critical and difficult to assess is the gas exchange coefficient. To date, there is no method totally satisfactory to quantify k in estuaries, and this question is still a matter of debate between biogeochemists, ecologists, and physicists (Borges and Abril, 2012). In their review the authors report an approx. range of $k_{600}$ of < 10 up to 30 cm/h (< 2.4 - 7.2 m/d). For the North Sea in winter much higher values are given (7 – 62 cm/h = 17 – 150 m/d) by Nightingale et al., (2000). Similar values are given for a Bay in the Baltic Sea with around 7

460    cm/h = 17 m/d (Silvennoinen et al., 2008). But lower values are reported for a Japanese estuary in summer (0.69 – 3.2 cm/h = 1.7 -7.7 m/d; (Tokoro et al., 2007). Our values for $k_{600}$ ranged from 0.37 to 3.17 m d$^{-1}$ with a median of 1.05 m d$^{-1}$. Thus our $k_{600}$ values lay within the lower range reported in literature.

With all the assumptions and additional data, we calculate a median diffusive methane flux of 24 $\mu$mol m$^2$ d$^{-1}$, ranging from 4 – 163 $\mu$mol m$^2$ d$^{-1}$. Our data lay well within the data reported from previous studies within this

465    area (Table 3) (Bussmann, 2013b; Shakhova and Semiletov, 2007). Wahlström and Meier (2014) applied a modelling approach, resulting in even lower methane fluxes (Table 3). In the North Sea the stratification of the water column in summer significantly reduced the diffusive methane flux, even at an active seep location (Mau et al., 2015). For the Baltic Sea, values are comparable to the North Sea (Steinle et al. 2017). The area off Svalbard is another polar region within the scientific focus. A comprehensive study by Myhre et al. (2016)

470    calculated a median methane flux of only 3 $\mu$mol m$^2$ d$^{-1}$, which is supported by a median methane flux of 2 $\mu$mol m$^2$ d$^{-1}$ for the coastal waters of Svalbard (Mau et al., 2017) and within the range of 4 – 20 $\mu$mol m$^2$ d$^{-1}$ (Graves et al., 2015) (Table 3). For the North American Arctic Ocean and its shelf seas rather low methane fluxes are reported (1.3 $\mu$mol m$^2$ d$^{-1}$, Fenwick et al. 2017). Our two stations with the high methane fluxes are similar to values reported for the North Sea with a mixed water column.

475    In contrast to these bottom-up calculations, very few studies focus on the atmospheric methane concentrations in this area (Thornton et al., 2016; Shakhova et al., 2014; Shakhova et al., 2010) or polar regions (Myhre et al., 2016). The resulting top-down calculations of the methane flux seem to be higher than the bottom-up calculations, with 94 and 200 – 300 $\mu$mol m$^2$ d$^{-1}$ (Thornton et al., 2016; Myhre et al., 2016) respectively. Ebullition of methane from the sediment in this area is also reported, resulting in very high methane fluxes 1 – 2

480    orders of magnitude higher than the other calculations (Table 3). The methane released by ebullition did not show any isotopic evidence of oxidation and thus will be released almost completely into the atmosphere (Sapart et al. 2017). However, if this ebullition really results in elevated atmospheric methane concentrations is a matter of debate, as this fingerprint was not detected by others (Thornton et al., 2016; Berchet et al., 2015). Overall the

East Siberian Arctic shelf seem to play an insignificant role in the methane emissions, compared to wetland and anthropogenic methane emissions in eastern Siberia (Berchet et al., 2015).

**4.4     Role of microbial methane oxidation versus diffusive methane flux**

To estimate the role of methane oxidation and diffusive methane flux for the methane inventory in the Lena Delta, we calculated the total methane inventory (details see Method section), as well as the total methane oxidation and total diffusive flux of this area. When the total methane inventory was set to 100%, then within one day a median of 1% (range 0.3 – 3.8%) was consumed by bacteria within the system, while a median of 8% (1 – 47%) left the system into the atmosphere. A similar estimation has been made by Mau et al., (2017) for the coastal waters of Svalbard. Here a much higher fraction of the dissolved methane (0.02-7.7%) was oxidized and only a minor fraction (0.07%) was transferred into the atmosphere. However, this region was much deeper, thus the ratio of water volume (including the methane oxidation activity) to the surface area (including the diffusive methane flux) was much bigger. Another polar study off Svalbard suggest that in the bottom water about 60% of the methane is oxidized, before it can mix with intermediate or surface water (Graves et al., 2015). For the coastal waters of the Baltic Sea, the given values for total MOX and total diffusive flux of the study were related to the total methane inventory. Accordingly, with a weakly or strongly stratified water column about 1.5 – 3.5% of the methane inventory were oxidized, while 0.2 – 5.2% diffused into the atmosphere, respectively (Steinle et al. 2017).

However, it has to be kept in mind that our estimation is a static one, which does not take into account the currents and spreading of the freshwater plume. In estuaries the residence time of the water (as influenced by water discharge and tidal force) also influences the efficiency of the estuarine filter (Bauer et al., 2013). The bulk of the freshwater from the Lena River stays in the eastern Laptev during the summer season (Fofonova et al., 2015). However, changing atmospheric conditions render the Laptev Sea Shelf highly time-dependent and turbulent (Heim et al., 2014). A more complex approach was performed by Wahlström and Meier (2014). Their simulations reveal the importance of the oxidation rate constant and crucial necessity to do in situ measurement of the oxidation rate constant. Beside the methane oxidation rate, the concentration of methane in the river runoff and the methane flux from the sediment are statistically significant important factors for the sea-air flux of methane (Wahlström and Meier, 2014).

**Conclusions**

In our study we could show that the methane sinks in the water column of the Lena Delta were rather weak, 1% of the methane inventory is oxidized per day and 8% diffuse into the atmosphere. Thus these water masses represent a strong methane source for the waters of the Laptev Sea and the central Arctic Ocean, but only to a limited extend as methane source to the atmosphere.

In context of the expected and ongoing warming of the Arctic regions, we would expect a different hydrographic regime i.e. more freshwater input and stronger stratification (Bring et al., 2016). With a greater proportion of riverine water there would be also more riverine MOBs. However, as this population is very divers, they will be able to adjust to a changing environment and respond well to increasing water temperatures. However, if a changed hydrography would result in a larger proportion of "mixed water", this would lead to an approx. 4fold reduction of MOX, as conditions in this water mass were not favourable for MOBs.

525 We could show no direct evidence of riverine import of methane. We assume that the process of ice formation and ice melting in the estuary modifies the freshwater signal in a complex way. Future studies should therefore assess the role of ice cover and ice formation in the Lena Delta on the methane cycle.

**Acknowledgments**

530 The authors acknowledge the Captain and the crew of the R/V "Dalnie Zelentsy". We are thankful to the logistics department of the Alfred Wegener Institute, particularly W. Schneider. Special thanks to N. Kasatkina and D. Moiseev from the Murmansk Marine Biological Institute for offering laboratory support. We also want to thank Ellen Damm for fruitful discussions and Patricia Tavormina for help in setting up the MISA. The methane related data set is available at www.pangaea.de, doi:10.1594/PANGAEA.868494, 2016.

**Figures and Tables**

Figure 1. Map of the study area in September 2013 and sampling locations, with four transects heading from near shore to about 120 km offshore (Transect 1).

Figure 2. Salinity (A, in PSU) and methane (B, in nmol L$^{-1}$)) distribution versus depth and distance from the shore for Transect 1. In (A) the water masses are also indicated defined as „riverine" with a salinity < 5, „mixed water" between 5 and 20, and „polar water" with a salinity > 20. The grey bars indicate the location of the stations. In (B) he pale orange indicates values above 150 nmol L$^{-1}$.

Figure 3. Methane concentrations in nmol L$^{-1}$ at the surface of the study area. The pale orange indicates values above 150 nmol L$^{-1}$ .

Figure 4. Correlation between the methane concentration in bottom water and the concentration in the underlying sediment for all stations (r$^2$ = 0.62, p < 0.001, n = 33). Two very high values from station TIII-1304 were excluded from the analysis.

Figure 5. Methane oxidation rates in nmol L$^{-1}$ d$^{-1}$ in surface (A) and bottom (B) water around the Lena Delta.

Figure 6. Relative abundance of methanotrophic DNA (as %MOB-DNA) in surface (A) and bottom (B) water around the Lena Delta

Appendix Figure A1. Map of study area with two grids to estimate the total sampling area.

Appendix Figure A2. Salinity in surface waters around the Lena Delta.

Table 1. The median values of important parameters in the different water masses. A one-way ANOVA was performed to test for significant differences of the log-transformed data between the water masses.

Table 2. Occurrence of the MISA OTUs in the different water masses and the results of a Kruskal Wallis test, if the differences in occurrence were significant (*).

Table 3. Comparison of diffusive methane flux of this region and other shelf seas (in $\mu$mol m$^2$ d$^{-1}$).

Appendix Table A1. Linear correlation between the methane concentration versus different environmental parameters splitted into three water masses. Analysis was performed with log transformed data, shown are the r$^2$-values and the level of significance (p).

Appendix Table A2. Linear correlation between the methane oxidation rate (MOX) and the fractional turnover rate (k) versus different environmental parameters splitted into three water masses. Analysis was performed with log transformed data, shown are the r$^2$-values and the level of significance (p). Empty fields indicate no significant correlation

**References**

Alin, S. R., de Fátima F. L. Rasera, M., Salimon, C. I., Richey, J. E., Holtgrieve, G. W., Krusche, A. V., and
      Snidvongs, A.: Physical controls on carbon dioxide transfer velocity and flux in low-gradient river
      systems and implications for regional carbon budgets, Journal of Geophysical Research G:
570      Biogeosciences, 116, G01009, doi:10.1029/2010jg001398, 2011.

Bauer, J. E., Cai, W. J., Raymond, P. A., Bianchi, T. S., Hopkinson, C. S., and Regnier, P. A. G.: The changing
      carbon cycle of the coastal ocean, Nature, 504, 61-70, 10.1038/nature12857, 2013.

Berchet, A., Pison, I., Chevallier, F., Paris, J. D., Bousquet, P., Bonne, J. L., Arshinov, M. Y., Belan, B. D.,
      Cressot, C., Davydov, D. K., Dlugokencky, E. J., Fofonov, A. V., Galanin, A., Lavrič, J., Machida, T.,
575      Parker, R., Sasakawa, M., Spahni, R., Stocker, B. D., and Winderlich, J.: Natural and anthropogenic
      methane fluxes in Eurasia: a mesoscale quantification by generalized atmospheric inversion, 12,
      5393-5414, doi:10.5194/bg-12-5393-2015, 2015.

Borges, A. V., and Abril, G.: Carbon Dioxide and Methane Dynamics in Estuaries, in: Treatise on estuarine
      and coastal science, edited by: Wolanski E, and DS, M., Academic Press, Waltham,, 119–161, 2012.

580    Bring, A., Fedorova, I., Dibike, Y., Hinzman, L., Mård, J., Mernild, S. H., Prowse, T., Semenova, O., Stuefer, S. L.,
      and Woo, M. K.: Arctic terrestrial hydrology: A synthesis of processes, regional effects, and research
      challenges, Journal of Geophysical Research: Biogeosciences, 121, 621-649,
      10.1002/2015JG003131, 2016.

Bussmann, I.: Methane release through suspension of littoral sediment, Biogeochem., 74, 283 - 302, 2005.

585    Bussmann, I.: Methane concentration and isotopic composition (d13C) in the waters of the Lena River and
      the Laptev Sea, in the years 2008, 2009 and 2010, www.pangaea.de,
      doi:10.1594/PANGAEA.817302, 2013a.

Bussmann, I.: Distribution of Methane in the Lena Delta and Buor Khaya Bay, Russia, Biogeosciences, 10,
      4641–4465, doi:10.5194/bg-10-4641-2013, 2013b.

590    Bussmann, I., Matousu, A., Osudar, R., and Mau, S.: Assessment of the radio 3H-CH$_4$ tracer technique to
      measure aerobic methane oxidation in the water column Limnol. Oceanogr.: Methods, 13, 312-327,
      doi:10.1002/lom3.10027, 2015.

Caspers, H.: Vorschläge einer Brackwassernomenklatur (The Venice System), Int. Rev. Ges. Hydrbiol., 44,
      313-316, 1959.

595    Damm, E., Rudels, B., Schauer, U., Mau, S., and Dieckmann, G.: Methane excess in Arctic surface water-
      triggered by sea ice formation and melting, Scientific Reports, 5, 16179, doi:10.1038/srep16179,
      2015.

DelSontro, T., Boutet, L., St-Pierre, A., del Giorgio, P. A., and Prairie, Y. T.: Methane ebullition and diffusion
      from northern ponds and lakes regulated by the interaction between temperature and system
600      productivity, Limnol. Oceanogr., n/a-n/a, 10.1002/lno.10335, 2016.

Dubinenkov, I., Kraberg, A. C., Bussmann, I., Kattner, G., and Koch, B. P.: Physical oceanography and
      dissolved organic matter in the coastal Laptev Sea in 2013, www.pangaea.de,
      doi:10.1594/PANGAEA.842221, 2015.

605 Eicken, H., Dmitrenko, I., Tyshko, K., Darovskikh, A., Dierking, W., Blahak, U., Groves, J., and Kassens, H.: Zonation of the Laptev Sea landfast ice cover and its importance in a frozen estuary, Global Planet. Change, 48, 55-83, doi.org/10.1016/j.gloplacha.2004.12.005, 2005.

Fenwick, L., Capelle, D., Damm, E., Zimmermann, S., Williams, W. J., Vagle, S., and Tortell, P. D.: Methane and nitrous oxide distributions across the North American Arctic Ocean during summer, 2015, Journal of Geophysical Research: Oceans, 122, 390-412, 10.1002/2016JC012493, 2017.

610 Florez-Leiva, L., Damm, E., and Farías, L.: Methane production induced by dimethylsulfide in surface water of an upwelling ecosystem, Prog. Oceanogr., 112–113, 38–48, 2013.

Fofonova, V., Danilov, S., Androsov, A., Janout, M., Bauer, M., Overduin, P., Itkin, P., and Wiltshire, K. H.: Impact of wind and tides on the Lena River freshwater plume dynamics in the summer season, Ocean Dynamics, 65, 951-968, doi:10.1007/s10236-015-0847-5, 2015.

615 Gentz, T., Damm, E., von Deimling, J. S., Mau, S., McGinnis, D. F., and Schlüter, M.: A water column study of methane around gas flares located at the West Spitsbergen continental margin, Cont. Shelf Res., doi:10.1016/j.csr.2013.07.013, 2013.

Gonçalves-Araujo, R., Stedmon, C. A., Heim, B., Dubinenkov, I., Kraberg, A., Moiseev, D., and Bracher, A.: From fresh to marine waters: characterization and fate of dissolved organic matter in the Lena
620 River delta region, Siberia, Frontiers in Marine Science, 2, 2015.

Graves, C. A., Steinle, L., Rehder, G., Niemann, H., Connelly, D. P., Lowry, D., Fisher, R. E., Stott, A. W., Sahling, H., and James, R. H.: Fluxes and fate of dissolved methane released at the seafloor at the landward limit of the gas hydrate stability zone offshore western Svalbard, Journal of Geophysical Research: Oceans, n/a-n/a, doi:10.1002/2015JC011084, 2015.

625 Hackbusch, S.: Abundance and activity of methane oxidizing bacteria in the River Elbe Estuary, Friedrich Schiller Universität Jena, 2014.

Heim, B., Abramova, E., Doerffer, R., Günther, F., Hölemann, J., Kraberg, A., Lantuit, H., Loginova, A., Martynov, F., Overduin, P. P., and Wegner, C.: Ocean colour remote sensing in the southern Laptev Sea: evaluation and applications, Biogeosciences, 11, 4191-4210, 10.5194/bg-11-4191-2014, 2014.

630 Ho, A., Kerckhof, F. M., Luke, C., Reim, A., Krause, S., Boon, N., and Bodelier, P. L. E.: Conceptualizing functional traits and ecological characteristics of methane-oxidizing bacteria as life strategies, Environmental Microbiology Reports, 5, 335-345, 10.1111/j.1758-2229.2012.00370.x, 2013.

Ho, A., de Roy, K., Thas, O., De Neve, J., Hoefman, S., Vandamme, P., Heylen, K., and Boon, N.: The more, the merrier: heterotroph richness stimulates methanotrophic activity, ISME J, 8, 1945-1948,
635 10.1038/ismej.2014.74, 2014.

Institute, A. a. A. R.: Electronic archive AARI term meteorological and upper-air observations Hydrometeorological Observatory (station) Tiksi for 1932 - 2015. St. Petersburg, 2016.

Kirschke, S., Bousquet, P., Ciais, P., Saunois, M., Canadell, J. G., Dlugokencky, E. J., Bergamaschi, P., Bergmann, D., Blake, D. R., Bruhwiler, L., Cameron-Smith, P., Castaldi, S., Chevallier, F., Feng, L.,
640 Fraser, A., Heimann, M., Hodson, E. L., Houweling, S., Josse, B., Fraser, P. J., Krummel, P. B., Lamarque, J. F., Langenfelds, R. L., Le Qu√©r√©, C., Naik, V., O'Doherty, S., Palmer, P. I., Pison, I., Plummer, D., Poulter, B., Prinn, R. G., Rigby, M., Ringeval, B., Santini, M., Schmidt, M., Shindell, D. T., Simpson, I. J., Spahni, R., Steele, L. P., Strode, S. A., Sudo, K., Szopa, S., Van Der Werf, G. R., Voulgarakis, A., Van

645      Weele, M., Weiss, R. F., Williams, J. E., and Zeng, G.: Three decades of global methane sources and sinks, Nature Geoscience, 6, 813-823, 2013.

Knief, C.: Diversity and habitat preferences of cultivated and uncultivated aerobic methanotrophic bacteria evaluated based on pmoA as molecular marker, Frontiers in Microbiology, 6, doi:10.3389/fmicb.2015.01346, 2015.

Kodina, L. A., Tokarev, V. G., Korobeinik, G. S., Vlasova, L. V., and Bogacheva, M. P.: Natural Background of
650      Hydrocarbon Gases (C1–C5) in the Waters of the Kara Sea, Geochemistry International, 49, 666–678, 2008.

Kolb, S., Knief, C., Stubner, S., and Conrad, R.: Quantitative detection of methanotrophs in soil by novel pmoA-Targeted real-time PCR assays, Appl. Environ. Microbiol., 69, 2423-2429, 2003.

Krause, S., Lüke, C., and Frenzel, P.: Methane source strength and energy flow shape methanotrophic
655      communities in oxygen-methane counter-gradients, Environmental Microbiology Reports, 4, 203-208, doi:10.1111/j.1758-2229.2011.00322.x, 2012.

Lammers, R. B., Shiklomanov, A. I., Vörösmarty, C. J., Fekete, B. M., and Peterson, B. J.: Assessment of contemporary Arctic river runoff based on observational discharge records, J. Geophys. Res., 106(D4), 3321–3334, 2001.

660      Lecher, A. L., Kessler, J., Sparrow, K., Garcia-Tigreros Kodovska, F., Dimova, N., Murray, J., Tulaczyk, S., and Paytan, A.: Methane transport through submarine groundwater discharge to the North Pacific and Arctic Ocean at two Alaskan sites, Limnol. Oceanogr., 61, S344-S355, 10.1002/lno.10118, 2016.

Liss, P. S. & Slater, P. G. Flux of gases across the air-sea interface. Nature 247, 181- 184 (1974).

Lofton, D., Whalen, S., and Hershey, A.: Effect of temperature on methane dynamics and evaluation of
665      methane oxidation kinetics in shallow Arctic Alaskan lakes, Hydrobiologia, 721, 209-222, doi:10.1007/s10750-013-1663-x, 2014.

Lucas, J., Wichels, A., and Gerdts, G.: Spatiotemporal variation of the bacterioplankton community in the German Bight: from estuarine to offshore regions, Helgol. Mar. Res., DOI 10.1186/s10152-016-0464-9, 2016.

670      Magen, C., Lapham, L. L., Pohlman, J. W., Marshall, K., Bosman, S., Casso, M., and Chanton, J. P.: A simple headspace equilibration method for measuring dissolved methane, Limnol. Oceanogr.: Methods, 12, 637-650, doi:10.4319/lom.2014.12.637, 2014.

Mau, S., Gentz, T., Körber, J. H., Torres, M. E., Römer, M., Sahling, H., Wintersteller, P., Martinez, R., Schlüter, M., and Helmke, E.: Seasonal methane accumulation and release from a gas emission site in the
675      central North Sea, Biogeosciences, 12, 5261-5276, doi:10.5194/bg-12-5261-2015, 2015.

Mau, S., Römer, M., Torres, M., Bussmann, I., Pape, T., Damm, E., Geprägs, P., Wintersteller, P., Hsu, J. C.-W., Loher, M., and Bohrmann, G.: Widespread methane seepage along the continental margin off Svalbard - from Bjørnøya to Kongsfjorden, Nature Scientific Reports, 7, 42997, 2017, doi: 10.1038/srep42997

680      Murrell, J. C., and Jetten, M. S. M.: The microbial methane cycle, Environmental Microbiology Reports, 1, 279-284, 10.1111/j.1758-2229.2009.00089.x, 2009.

Myhre, C. L., Ferré, B., Platt, S. M., Silyakova, A., Hermansen, O., Allen, G., Pisso, I., Schmidbauer, N., Stohl, A., Pitt, J., Jansson, P., Greinert, J., Percival, C., Fjaeraa, A. M., O'Shea, S. J., Gallagher, M., Breton, M. L.,

685    Bower, K. N., Bauguitte, S. J. B., Dalsøren, S., Vadakkepuliyambatta, S., Fisher, R. E., Nisbet, E. G., Lowry, D., G.Myhre, Pyle, A., Cain, M., and Mienert, J.: Extensive release of methane from Arctic seabed west of Svalbard during summer 2014 does not influence the atmosphere, Geophys. Res. Lett., 43, 4624–4631, doi:10.1002/2016GL068999, 2016.

Nightingale, P. D., Malin, G., Law, C. S., Watson, A. J., Liss, P. S., Liddicoat, M. I., Boutin, J., and Upstill-Goddard, R. C.: In situ evaluation of air-sea gas exchange parameterizations using novel

690    conservative and volatile tracers, Glob. Biogeochem. Cycl., 14, 373-387, doi:10.1029/1999GB900091, 2000.

Nisbet, E. G., Dlugokencky, E. J., and Bousquet, P.: Methane on the rise - Again, Science, 343, 493-495, doi:10.1126/science.1247828, 2014.

Osudar, R., Matoušů, A., Alawi, M., Wagner, D., and Bussmann, I.: Environmental factors affecting methane

695    distribution and bacterial methane oxidation in the German Bight (North Sea), Estuar. Coast. Shelf Sci., 160, 10-21, doi:10.1016/j.ecss.2015.03.028, 2015.

Osudar, R., Liebner, S., Alawi, M., Yang, S., Bussmann, I., and Wagner, D.: Methane turnover and methanotrophic communities in arctic aquatic ecosystems of the Lena Delta, Northeast Siberia, FEMS Microbiol Ecol, doi: 10.1093/femsec/fiw116, 2016.

700    Osudar, R., Klings, K., Wagner, D., and Bussmann, I.: Effect of salinity on microbial methane oxidation in freshwater and marine environments, Aquat. Microb. Ecol., in revision.

Overduin, P. P., Liebner, S., Knoblauch, C., Gunther, F., Wetterich, S., Schirrmeister, L., Hubberten, H. W., and Grigoriev, M. N.: Methane oxidation following submarine permafrost degradation: Measurements from a central Laptev Sea shelf borehole, Journal of Geophysical Research-

705    Biogeosciences, 120, 965-978, doi:10.1002/2014jg002862, 2015.

Rachold, V., Bolshiyanov, D. Y., Grigoriev, M. N., Hubberten, H. W., Junker, R., Kunitsky, V. V., Merker, F., Overduin, P. P., and Schneider, W.: Near-shore Arctic Subsea Permafrost in Transition, EOS: Transactions of the American Geophysical Union, 88, 149-156, 2007.

Saunois, M., Bousquet, P., Poulter, B., Peregon, A., Ciais, P., Canadell, J. G., Dlugokencky, E. J., Etiope, G.,

710    Bastviken, D., Houweling, S., Janssens-Maenhout, G., Tubiello, F. N., Castaldi, S., Jackson, R. B., Alexe, M., Arora, V. K., Beerling, D. J., Bergamaschi, P., Blake, D. R., Brailsford, G., Brovkin, V., Bruhwiler, L., Crevoisier, C., Crill, P., Covey, K., Curry, C., Frankenberg, C., Gedney, N., Höglund-Isaksson, L., Ishizawa, M., Ito, A., Joos, F., Kim, H. S., Kleinen, T., Krummel, P., Lamarque, J. F., Langenfelds, R., Locatelli, R., Machida, T., Maksyutov, S., McDonald, K. C., Marshall, J., Melton, J. R., Morino, I., Naik, V.,

715    O'Doherty, S., Parmentier, F. J. W., Patra, P. K., Peng, C., Peng, S., Peters, G. P., Pison, I., Prigent, C., Prinn, R., Ramonet, M., Riley, W. J., Saito, M., Santini, M., Schroeder, R., Simpson, I. J., Spahni, R., Steele, P., Takizawa, A., Thornton, B. F., Tian, H., Tohjima, Y., Viovy, N., Voulgarakis, A., van Weele, M., van der Werf, G. R., Weiss, R., Wiedinmyer, C., Wilton, D. J., Wiltshire, A., Worthy, D., Wunch, D., Xu, X., Yoshida, Y., Zhang, B., Zhang, Z., and Zhu, Q.: The global methane budget 2000–2012, Earth Syst.

720    Sci. Data, 8, 697-751, 10.5194/essd-8-697-2016, 2016.

Sapart, C. J., Shakhova, N., Semiletov, I., Jansen, J., Szidat, S., Kosmach, D., Dudarev, O., van der Veen, C., Egger, M., Sergienko, V., Salyuk, A., Tumskoy, V., Tison, J.-L., and Röckmann, T.: The origin of

methane in the East Siberian Arctic Shelf unraveled with triple isotope analysis, Biogeosciences, 14, 2283-2292, 10.5194/bg-14-2283-2017, 2017, 2017.

725 Savvichev, A. S., Zakharova, E. E., Veslopolova, E. F., Rusanov, I. I., Lein, A. Y., and Ivanov, M. V.: Microbial processes of the carbon and sulfur cycles in the Kara Sea, Oceanology, 50, 893-908, 10.1134/S0001437010060093, 2010.

Schaal, P.: Diversity of methanotrophic bacteria in the Elbe Estuary, Master thesis, Hochschule Bremerhaven, Bremerhaven, 2016.

730 Schmale, O., Leifer, I., Deimling, J. S. V., Stolle, C., Krause, S., Kießlich, K., Frahm, A., and Treude, T.: Bubble Transport Mechanism: Indications for a gas bubble-mediated inoculation of benthic methanotrophs into the water column, Cont. Shelf Res., 103, 70-78, doi:10.1016/j.csr.2015.04.022, 2015.

Shakhova, N., and Semiletov, I.: Methane release and coastal environment in the East Siberian Arctic shelf, J. Mar. Syst., 66, 227-243, 2007.

735 Shakhova, N., Semiletov, I., Leifer, I., Salyuk, A., Rekant, P., and Kosmach, D.: Geochemical and geophysical evidence of methane release over the East Siberian Arctic Shelf, Journal of Geophysical Research: Oceans, 115, C08007, doi:10.1029/2009jc005602, 2010.

Shakhova, N., Semiletov, I., Leifer, I., Sergienko, V., Salyuk, A., Kosmach, D., Chernykh, D., Stubbs, C., Nicolsky, D., Tumskoy, V., and Gustafsson, O.: Ebullition and storm-induced methane release from 740 the East Siberian Arctic Shelf, Nature Geosci, 7, 64-70, 2014.

Silvennoinen, H., Liikanen, A., Rintala, J., and Martikainen, P.: Greenhouse gas fluxes from the eutrophic Temmesjoki River and its Estuary in the Liminganlahti Bay (the Baltic Sea), Biogeochem., 90, 193-208, doi:10.1007/s10533-008-9244-1, 2008.

Stanley, E. H., Casson, N. J., Christel, S. T., Crawford, J. T., Loken, L. C., and Oliver, S. K.: The ecology of 745 methane in streams and rivers: patterns, controls,and global significance, Ecol. Monogr., 86, 146-171, 2016.

Steinle, L., Graves, C. A., Treude, T., Ferre, B., Biastoch, A., Bussmann, I., Berndt, C., Krastel, S., James, R. H., Behrens, E., Boning, C. W., Greinert, J., Sapart, C.-J., Scheinert, M., Sommer, S., Lehmann, M. F., and Niemann, H.: Water column methanotrophy controlled by a rapid oceanographic switch, Nature 750 Geoscience, 8, 378–382, doi:10.1038/ngeo2420, 2015.

Steinle, L., Maltby, J., Treude, T., Kock, A., Bange, H. W., Engbersen, N., Zopfi, J., Lehmann, M. F., and Niemann, H.: Effects of low oxygen concentrations on aerobic methane oxidation in seasonally hypoxic coastal waters, Biogeosciences, 14, 1631-1645, 10.5194/bg-14-1631-2017, 2017.

Striegl, R. G., Dornblaser, M. M., McDonald, C. P., Rover, J. R., and Stets, E. G.: Carbon dioxide and methane 755 emissions from the Yukon River system, Glob. Biogeochem. Cycl., 26, doi:10.1029/2012GB004306, 2012.

Tavormina, P. L., Ussler, W., III, and Orphan, V. J.: Planktonic and sediment-associated aerobic methanotrophs in two seep systems along the North American margin, Appl. Environ. Microbiol., 74, 3985-3995, doi:10.1128/aem.00069-08, 2008.

760 Tavormina, P. L., Ussler, W., Joye, S. B., Harrison, B. K., and Orphan, V. J.: Distributions of putative aerobic methanotrophs in diverse pelagic marine environments, ISME J, 4, 700-710, 2010.

Thornton, B. F., Geibel, M. C., Crill, P. M., Humborg, C., and Mörth, C.-M.: Methane fluxes from the sea to the atmosphere across the Siberian shelf seas, Geophys. Res. Lett., 43, doi:10.1002/2016GL068977, 2016.

765 Tokoro, T., Watanabe, A., Kayanne, H., Nadaoka, K., Tamura, H., Nozaki, K., Kato, K., and Negishi, A.: Measurement of air-water $CO_2$ transfer at four coastal sites using a chamber method, J. Mar. Syst., 66, 140-149, doi:10.1016/j.jmarsys.2006.04.010, 2007.

Wahlström, I., and Meier, H. E. M.: A model sensitivity study for the sea–air exchange of methane in the Laptev Sea, Arctic Ocean, Tellus B, 66, 24174,, doi.org/10.3402/tellusb.v66.24174, 2014.

770 Wanninkhof, R., Asher, W. E., Ho, D. T., Sweeney, C. S., and McGillis, W. R.: Advances in quantifying air-sea gas exchange and environmental forcing, Annual Review of Marine Science (2009), 1, 213-244, doi:10.1146/annurev.marine.010908.163742, 2009.

Wanninkhof, R.: Relationship between wind speed and gas exchange over the ocean revisited, Limnol. Oceanogr.: Methods, 12, 351-362, doi:10.4319/lom.2014.12.351, 2014.

775 Westbrook, G. K., Thatcher, K. E., Rohling, E. J., Piotrowski, A. M., Pälike, H., Osborne, A. H., Nisbet, E. G., Minshull, T. A., Lanoiselle, M., James, R. H., Hühnerbach, V., Green, D., Fisher, R. E., Crocker, A. J., Chabert, A., Bolton, C., Beszczynska-Möller, A., Berndt, C., and Aquilina, A.: Escape of methane gas from the seabed along the West Spitsbergen continental margin, Geophys. Res. Lett., 36, L15608, doi:10.1029/2009GL039191, 2009.

780 Wiesenburg, D. A., and Guinasso, N. L.: Equilibrium solubilities of methane, carbon monoxide and hydrogen in water and sea water, J. Chem. Eng. Data, 24, 356-360, 1979.
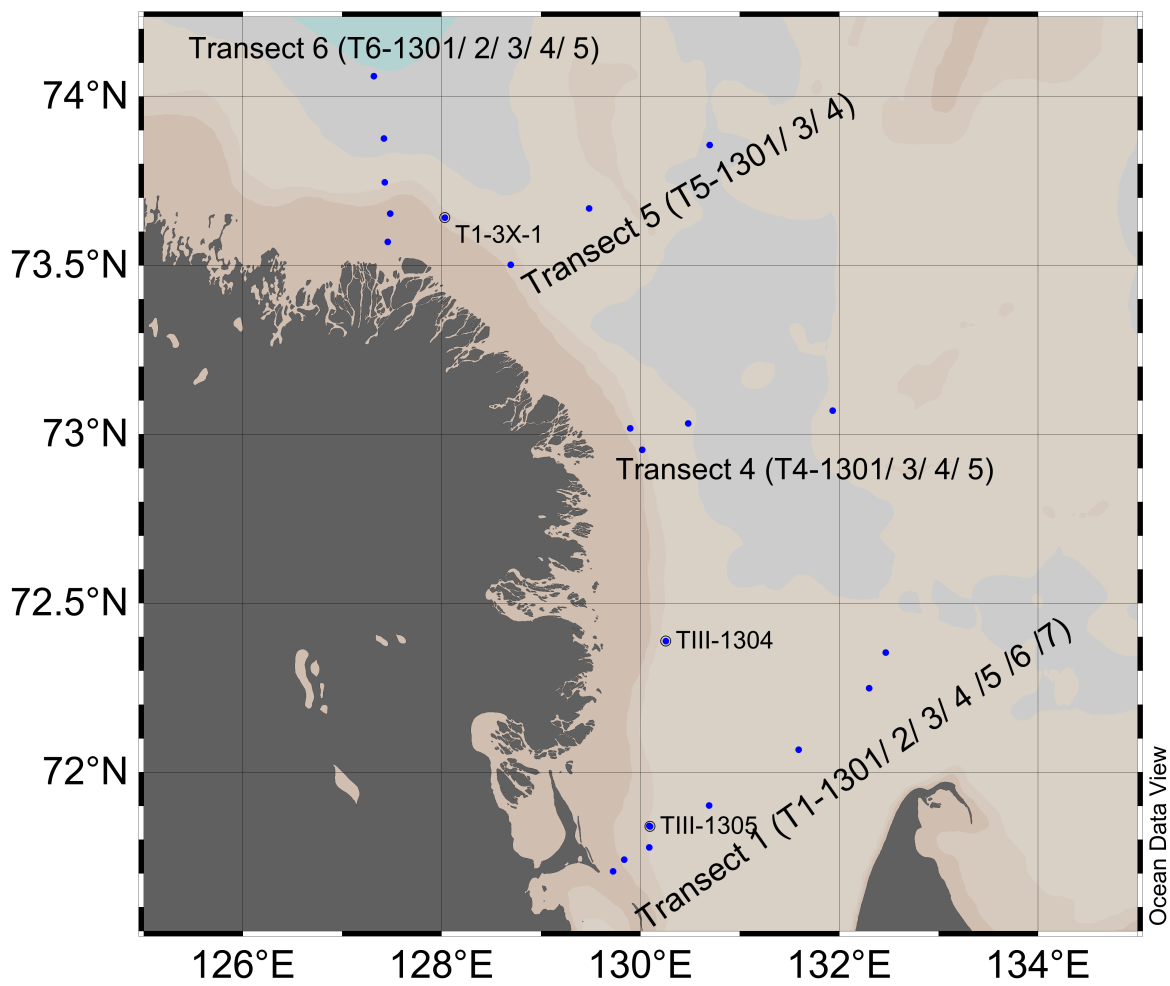
**Figure 1. Map of the study area in September 2013 and sampling locations, with four transects heading from near shore to about 120 km offshore (Transect 1).**

**A**

**B**
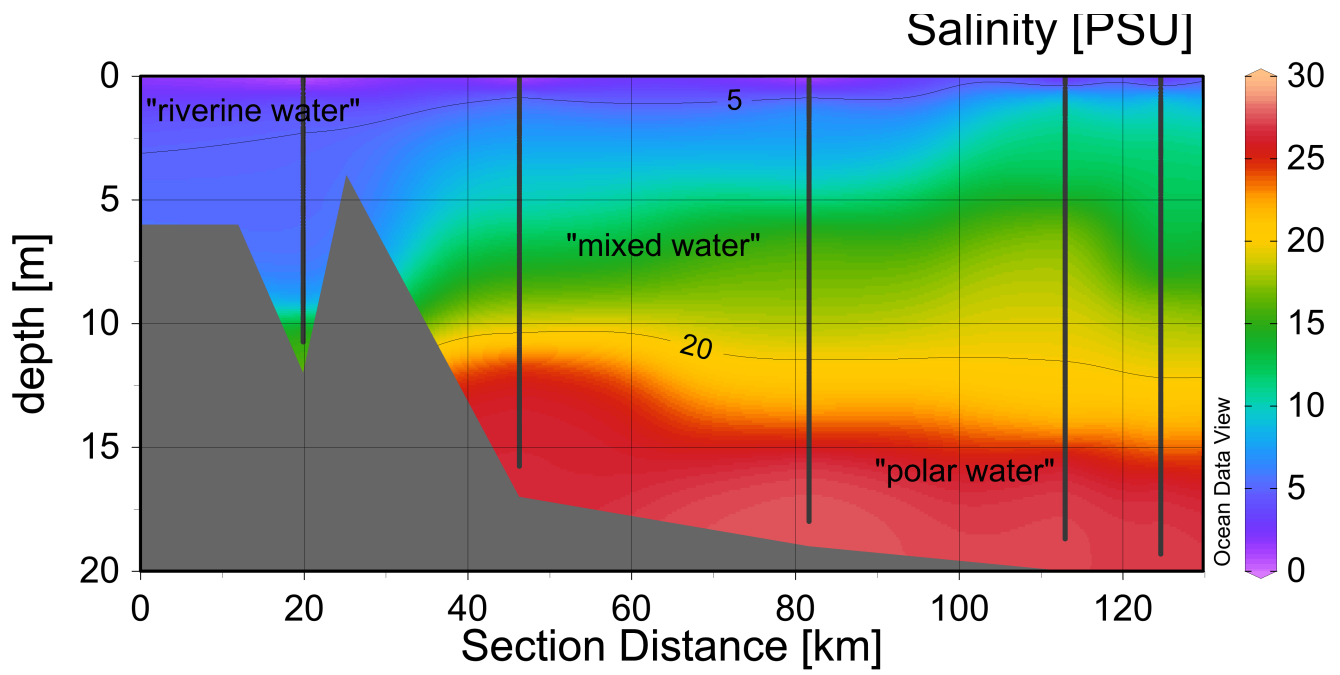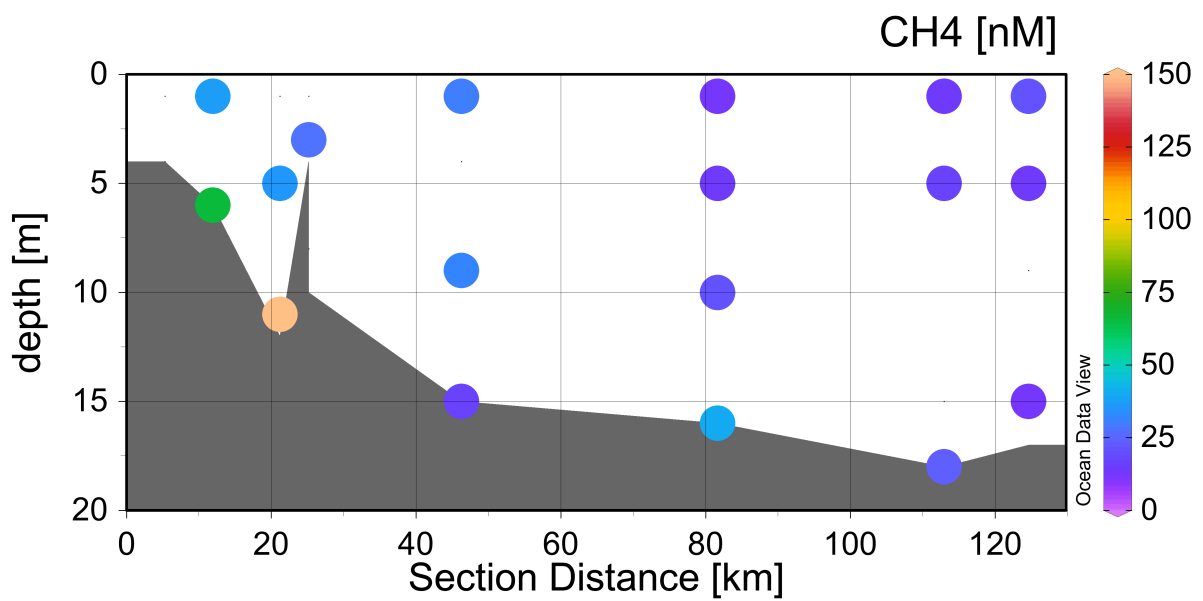
**Figure 2. Salinity (A, in PSU) and methane (B, in nmol L$^{-1}$)) distribution versus depth and distance from the shore for Transect 1. In (A) the water masses are also indicated defined as „riverine" with a salinity < 5, „mixed water" between 5 and 20, and „polar water" with a salinity > 20. The grey bars indicate the location of the stations. In (B) he pale orange indicates values above 150 nmol L$^{-1}$.**
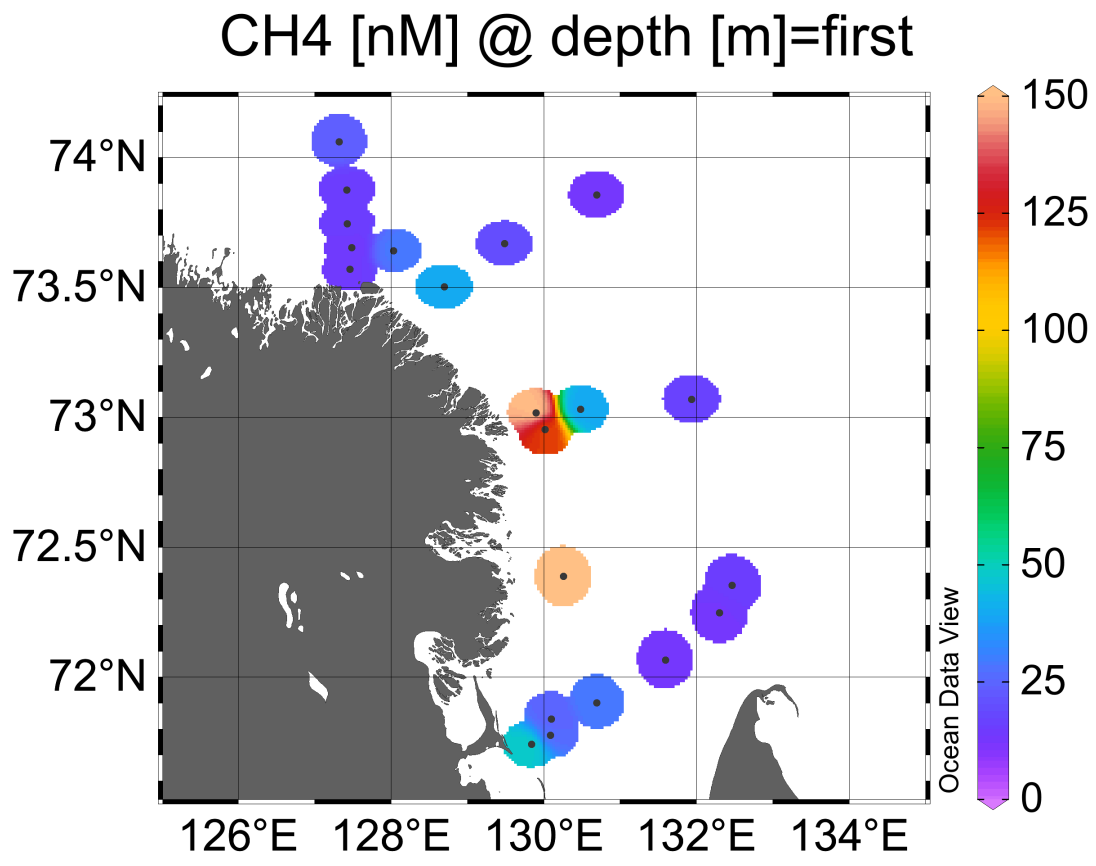
800

**Figure 3. Methane concentrations in nmol L$^{-1}$ at the surface of the study area. The pale orange indicates values above 150 nmol L$^{-1}$ .**
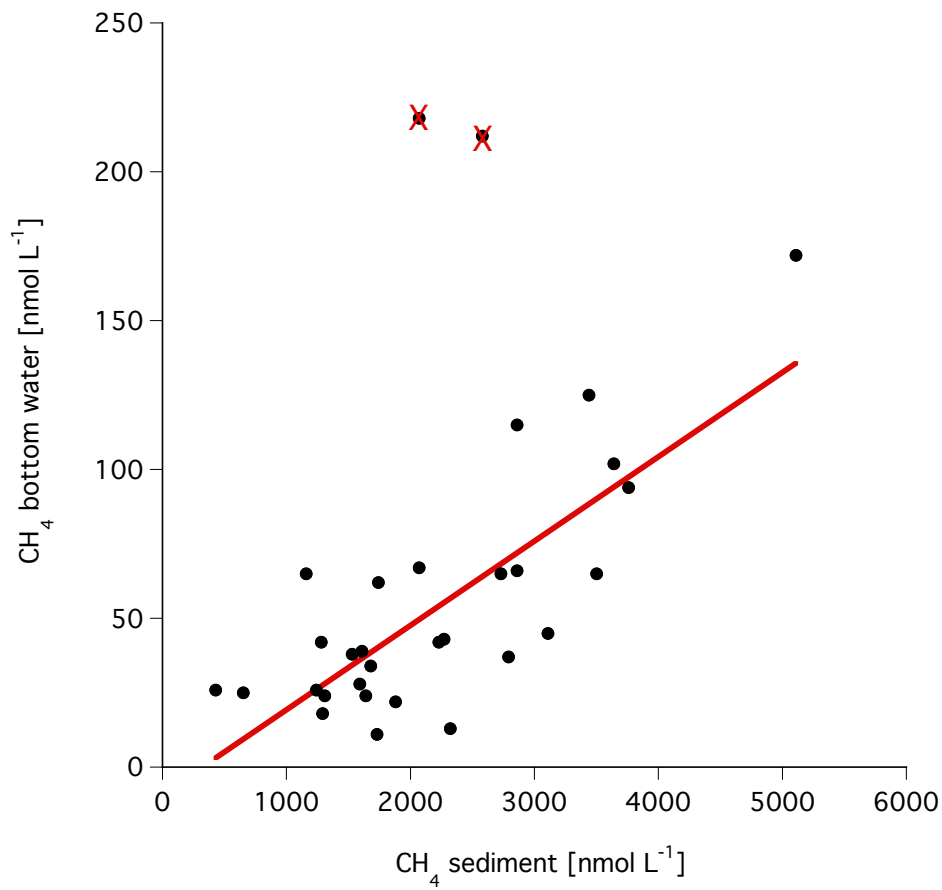
805     **Figure 4. Correlation between the methane concentration in bottom water and the concentration in the underlying sediment for all stations (r2 = 0.62, p < 0.001, n= 33). Two very high values from station TIII-1304 were excluded from the analysis.**

810 **A**

**B**

**Figure 5. Methane oxidation rates in nmol L$^{-1}$ d$^{-1}$ in surface (A) and bottom (B) water around the Lena**

815 **Delta.**

**A**

820 **B**

**Figure 6. Relative abundance of methanotrophic DNA (as %MOB-DNA) in surface (A) and bottom (B) water around the Lena Delta**

median depth 13 m
area: $1.02 \times 10^{10}$ m$^2$
volume: $1.33 \times 10^{11}$ m$^3$

median depth 13 m
area: $2.01 \times 10^{10}$ m$^2$
volume: $2.52 \times 10^{11}$ m$^3$

Ocean Data View
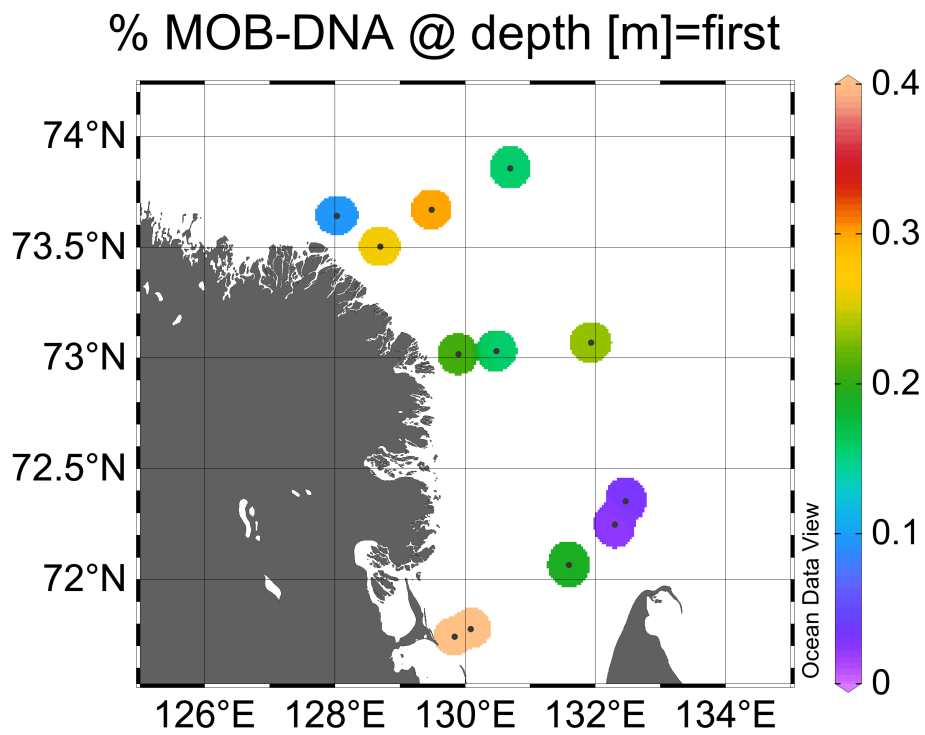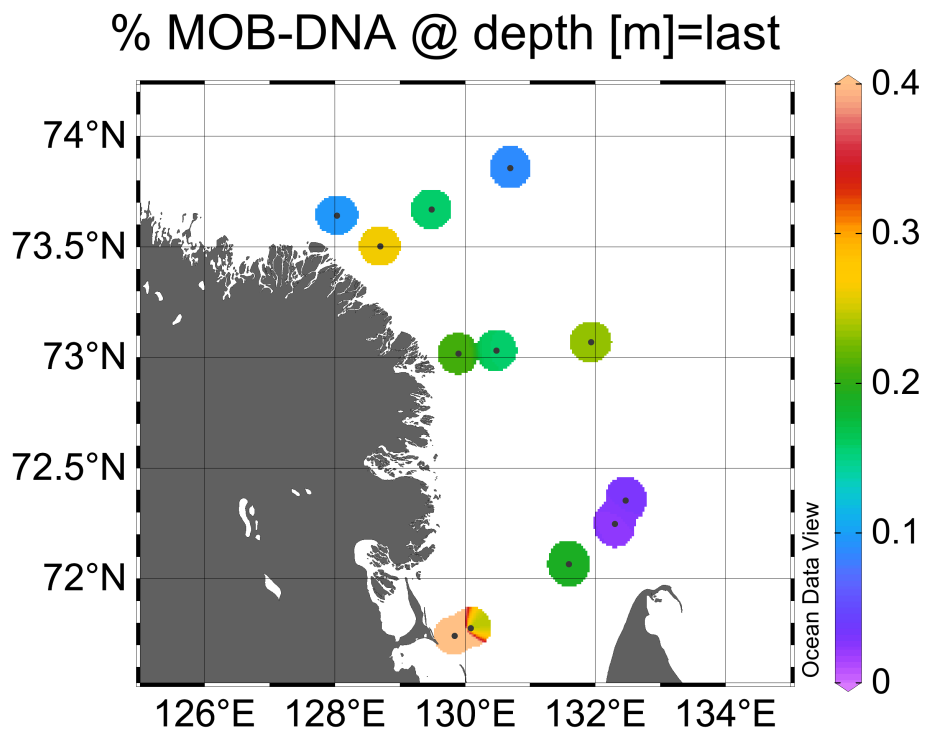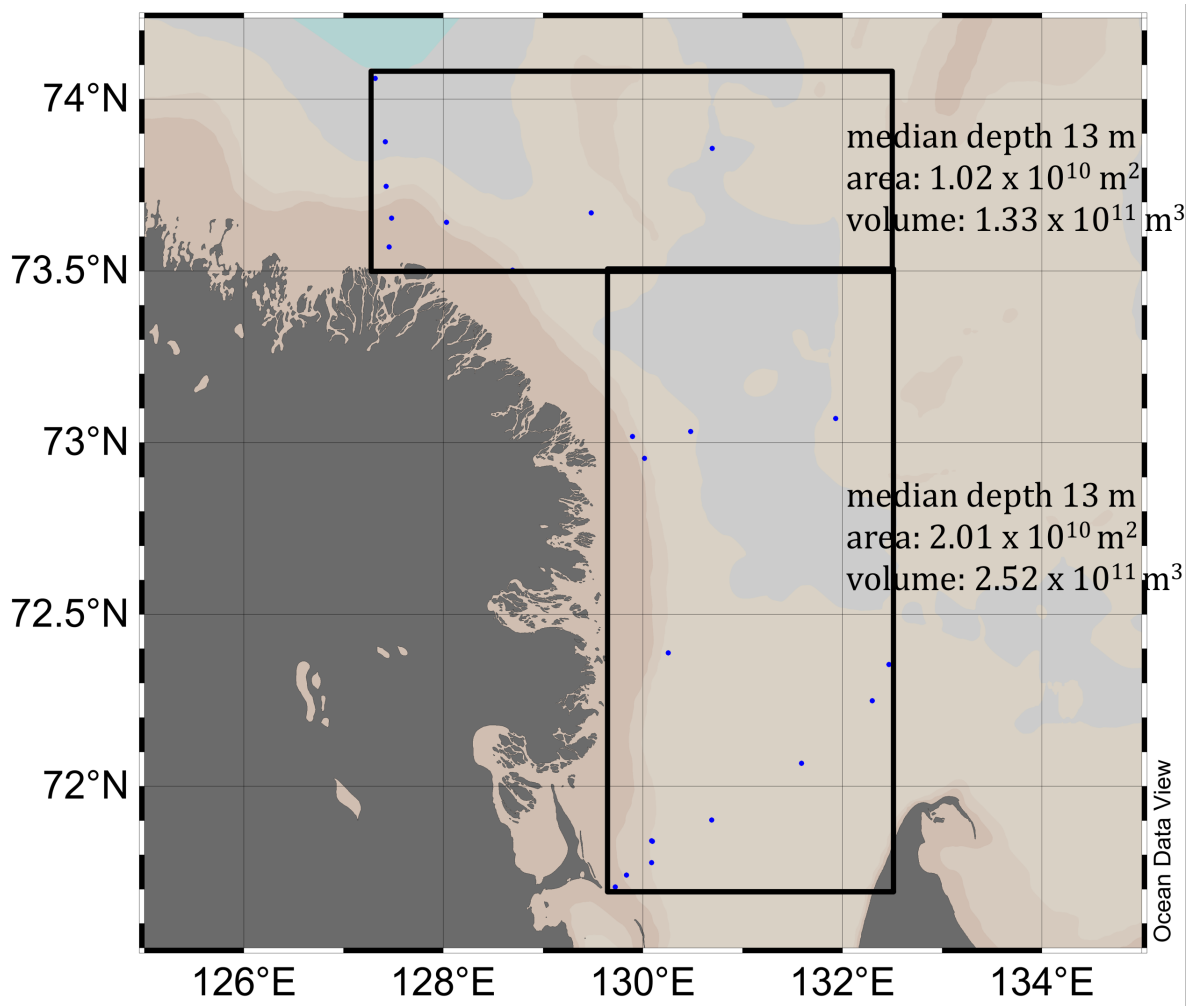
825

**Appendix Figure A1. Map of study area with two grids to estimate the total sampling area.**

**Appendix Figure A2. Salinity in surface waters around the Lena Delta.**

830
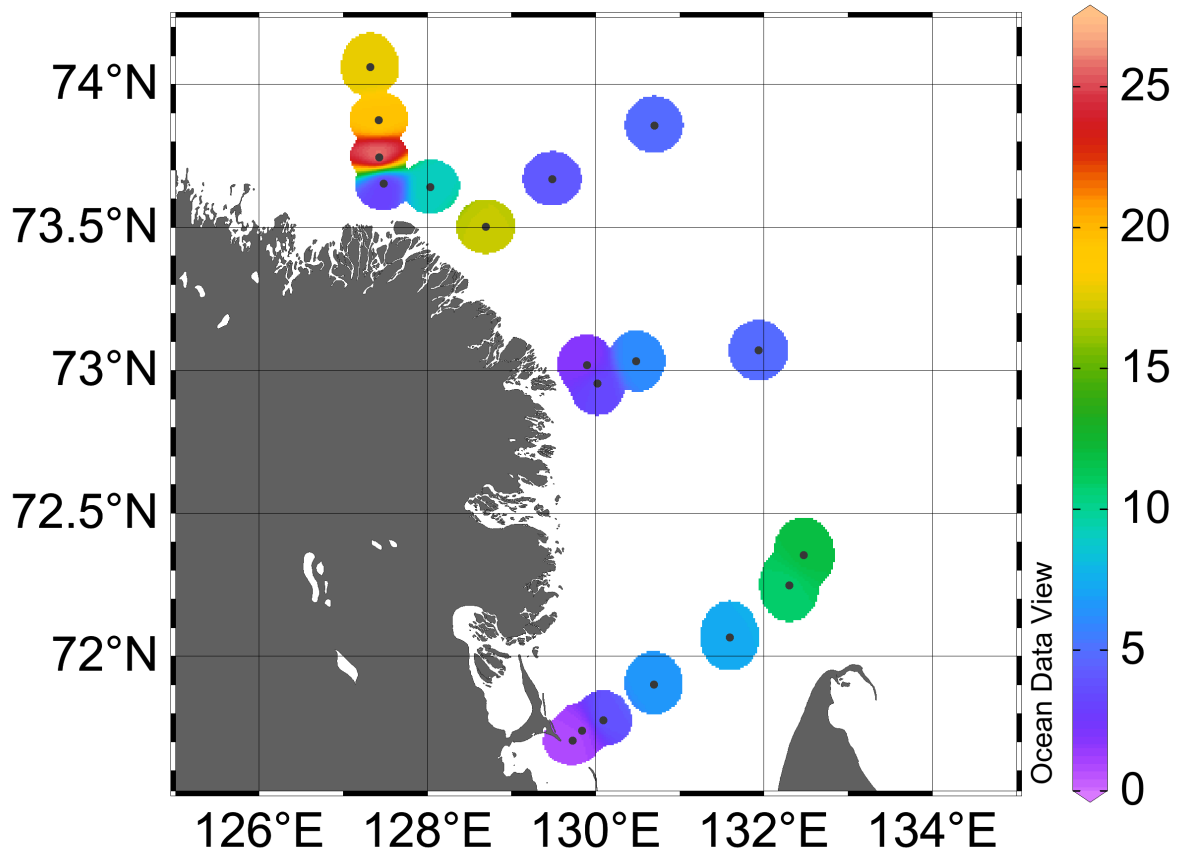
**Table 1. The median values of important parameters in the different water masses. A one-way ANOVA was performed to test for significant differences of the log-transformed data between the water masses.**

| | Median for „riverine water" | Median for „mixed water" | Median for „polar water" | DF / p |
|---|---|---|---|---|
| $CH_4$ [nmol $L^{-1}$] | 22 | 19 | 26 | **94 / 0.03 \*** |
| MOX [nmol $L^{-1}$ $d^{-1}$] | 0.419 | 0.089 | 0.400 | 68 / 0.18 |
| k' [d] | 0.011 | 0.006 | 0.028 | **68 / < 0.001 \*\*\*** |
| Turnover time (d) | 91 | 167 | 36 | |
| %MOB | 0.81 | 0.19 | 0.03 | **23 / <0.001 \*\*\*** |
| "estimated diversity" [OTUs / station] | 4 | 3 | 2 | **23 / 0.01 \*\*** |

835

**Table 2. Occurrence of the MISA OTUs in the different water masses and the results of a Kruskal Wallis test, if the differences in occurrence were significant (\*).**

| MISA OTU | assignation | Riverine | Mixed | Polar | Kruskal Wallis | Association |
|---|---|---|---|---|---|---|
| OTU-557 | | 3 | 3 | **9** | 0.06 | Polar |
| OTU-535 | Group Z \*\* | **6** | **6** | 3 | **0.02 \*** | River /mixed |
| OTU-485 | *Methylococcus capsulatus* \*\*\* | 3 | 2 | 2 | 0.4 | |
| OTU-460 | | **3** | **3** | 0 | 0.06 | River /mixed |
| OTU-445 | OPU-1 \*\* | 4 | 3 | 4 | 0.5 | |
| OTU-398 | | **1** | 0 | 0 | 0.2 | River |
| OTU-362 | | **4** | **5** | 2 | 0.1 | River /mixed |
| Median number of OTUs / sample | | 6 | 5 | 4 | **0.02\*** | |

840    \*\* assignment according to Tavormina et al., (2010)

\*\*\* assignation according to Schaal, (2016)

**Table 3. Comparison of diffusive methane flux of this region and other shelf seas (in µmol m² d⁻¹).**

| Authors | Area | Range | Median |
|---|---|---|---|
| Calculated from dissolved methane concentrations (bottom-up) | | | |
| This study | Lena Delta<br><br>(2 coastal stations of Transect 4) | 4 – 163 | 24<br><br>536 |
| (Bussmann, 2013b) | Buor Kaya Bay | 2 -85 | 34 |
| (Shakhova and Semiletov, 2007) | Northern parts of Buor-Khaya Bay | 4 – 8 | |
| (Wahlström and Meier, 2014) | Modelled flux for Laptev Sea | 6 ± 1 | |
| (Mau et al., 2015) | North Sea with stratified water column in summer | 2 -35 | 9 |
| (Mau et al., 2015) | North Sea in winter, including methane seepage | 52 - 544 | 104 |
| (Steinle et al., 2017) | Eckernförde Bay, Baltic Sea | 6 - 15 | 8 |
| (Myhre et al., 2016) | West off Svalbard with $CH_4$ seepage. | Up to 69 | 3 |
| (Mau et al., 2017) | Coastal waters of Svalbard | -17 – 173 | 2 |
| (Graves et al., 2015) | Coastal waters of Svalbard | 4 - 20 | |
| (Fenwick et al., 2017) | North American Arctic Ocean | -0.4 – 4.9 | 1.3 |
| Calculated, modelled from atmospheric data (top-down) | | | |
| (Thornton et al., 2016) | ice free Laptev Sea | | 94 |
| (Myhre et al., 2016) | West off Svalbard with $CH_4$ seepage | 207 - 328 | |
| | | | |
| (Shakhova et al., 2014) | Ebullitive flux around Lena Delta | 6250 - 39375 | |

845

Appendix Table A1. Linear correlation between the methane concentration versus different environmental parameters splitted into three water masses. Analysis was performed with log transformed data, shown are the $r^2$-values, the level of significance (p) and the positive or negative correlation (+/-).

| | „Riverine water" (n = 13) | „mixed water" (n = 22) | „polar water" (n = 24) |
|---|---|---|---|
| Temperature | 5  (+) 0.38 / 0.02 | (+) 0.003 / 0.74 | (-) 0.10 / 0.04 |
| Salinity | (-) 0.23 / 0.13 | (+) 0.03 / 0.25 | (-) 0.0001 / 0.93 |
| $O_2$ | 6  (-) 0.73 / <0.001 | (-) 0.02 / 0.36 | (-) 0.006 / 0.65 |
| DOC | (+) 0.002 / 0.89 | (+) 0.01 / 0.31 | (-) 0.0003 / 0.94 |
| TDN | (-) 0.0006 / 0.95 | 7  (+) 0.27 / 0.01 | (+) 0.11 / 0.12 |
| Sediment $CH_4$ | n.d. | n.d. | 8  (+) 0.33 / < 0.001 |

n.d. not determined because not enough data points

Appendix Table A2. Linear correlation between the methane oxidation rate (MOX) and the fractional turnover rate (k') versus different environmental parameters splitted into three water masses. Analysis was performed with log transformed data, shown are the $r^2$-values and the level of significance (p). Empty fields indicate no significant correlation

| | „Riverine water" (n = 6) | | „mixed water" (n = 9) | | „polar water" (n = 11) | |
|---|---|---|---|---|---|---|
| | MOX | k' | MOX | k' | MOX | k' |
| Temperature | 9 (+) 0.77 / 0.02 | 10 (+) 0.84 / 0.01 | (+) 0.01 / 0.77 | (+) 0.004 / 0.87 | (-) 0.02 / 0.69 | (-) 0.07 / 0.41 |
| Salinity | (-) 0.30 / 0.26 | (-) 0.43 / 0.16 | (+) 0.30 / 0.12 | 0.46 / 0.04 | (+) 0.05 / 0.52 | (+) 0.17 / 0.21 |
| $O_2$ | (-) 0.33/0.23 | (-) 0.30 / 0.26 | (-) 0.006 / 0.83 | (-) 0.07 / 0.48 | (-) 0.03 / 0.67 | (-) 0.001 / 0.92 |
| DOC | (+) 0.29 /0.27 | (+) 0.46 / 0.14 | (-) 0.009 / 0.80 | (+) 0.02 / 0.75 | (+) 0.004 / 0.85 | (+) 0.007 / 0.80 |
| TDN | (-) 0.02 /0.80 | (-) 0.002 / 0.93 | (+) 0.30 / 0.13 | 11 (+) 0.37 / 0.08 | 12 (+) 0.31 / 0.08 | (+) 0.21 / 0.16 |
| Methane | 13 (+) 0.98 / <0.001 | 14 (+) 0.96 / <0.001 | 15 (+) 0.80 / < 0.001 | 16 (+) 0.73 / <0.001 | 17 (+) 0.56 / 0.01 | (+) 0.13 / 0.31 |